AN EXPERIMENTAL STUDY OF ELECTRODELESS ARC DISCHARGES

Dennis R. Keefer
University of Florida,
Gainesville, Florida

September 1971

ARNOLD ENGINEERING DEVELOPMENT CENTER
AIR FORCE SYSTEMS COMMAND
ARNOLD AIR FORCE STATION, TENNESSEE

NOTICES

When U. S. Government drawings specifications, or other data are used for any purpose other than a definitely related Government procurement operation, the Government thereby incurs no responsibility nor any obligation whatsoever, and the fact that the Government may have formulated, furnished, or in any way supplied the said drawings, specifications, or other data, is not to be regarded by implication or otherwise, or in any manner licensing the holder or any other person or corporation, or conveying any rights or permission to manufacture, use, or sell any patented invention that may in any way be related thereto.

Qualified users may obtain copies of this report from the Defense Documentation Center.

References to named commercial products in this report are not to be considered in any sense as an endorsement of the product by the United States Air Force or the Government.

AN EXPERIMENTAL STUDY OF ELECTRODELESS ARC DISCHARGES

Dennis R. Keefer
University of Florida,
Gainesville, Florida

FOREWORD

The work reported herein was sponsored by Arnold Engineering Development Center (AEDC), Air Force Systems Command (AFSC), Arnold Air Force Station, Tennessee, under Program Element 62201F, Project 8952, Task 08.

The results of research were obtained by the Aerospace Engineering Department, University of Florida, during the period from November 1969 to January 1971, under Contract F40600-70-C-0003. The report was submitted 15 July 1971 for publication.

The author would like to thank Dr. W. K. McGregor, Jr., and Mr. J. D. Few, ARO, Inc., for their suggestions regarding the spectroscopic measurements and Mr. C. C. Limbaugh, ARO, Inc., for his aid in the Abel inversion program. Dr. Erich Soehngen suggested the use of the bluff body as a stabilizer. The author would also like to thank graduate students D. J. Green for the photograph in Figure 5, and P. J. Gross and J. C. J. C. Swingle for their aid in the experimental effort.

The reproducibles used in the reproduction of this report were supplied by the authors.

This technical report has been reviewed and is approved.

M. A. Clermont
Captain, CF
Research & Development Division
Directorate of Technology

Robert O. Dietz
Acting Director
Directorate of Technology

ABSTRACT

An experimental study of electrodeless discharges, stabilized in a flowing stream, has shown that a substantial improvement in stability can be accomplished by the use of a bluff body placed in the entering flow. The increased stability is attributed to energy convection by the circulation cell formed in the wake of the bluff body. Spectroscopic measurements indicate that a more uniform temperature profile is produced as a result of the convective mixing. Detailed measurements indicate that a stable discharge can be maintained with flow rates 3 times greater than is possible with vortex stabilization. It was further determined that the gas heating efficiency of the device is increased by an order of magnitude when compared to the vortex stabilized discharge. The efficiency was found to increase with both power input and flow rate with no indication of a leveling off up to the maximum of 18% measured in the course of the study. A large discharge chamber was constructed to permit operation at pressures to ten atmospheres and input powers to 400 KW, but only preliminary experiments were performed.

TABLE OF CONTENTS

APPENDICES

TABLE OF CONTENTS, Continued

Figure

TABLE OF CONTENTS, Continued

Figure

NOMENCLATURE

a	Discharge radius
A	Orifice cross sectional area
A_{ij}	Transition probability
B	$\log\left(\frac{\varepsilon\lambda}{A_{ij}g_i}\right)$
C	Velocity of light
C_d	Orifice discharge coefficient
d	Orifice diameter
g	Statistical weight
h	Planck's constant
k	Boltzmann's constant
m	Mass flow rate
N	Number density
p	Pressure
R	Gas constant
T	Temperature
Z	Partition function
r	Ratio of specific heats
δ	Electrical skin depth
ϵ	Energy of an excited state
ε	Emission coefficient
λ	Wavelength
μ	Permeability
ν	Frequency

NOMENCLATURE, Continued

σ	Electrical conductivity
ω	Angular frequency

Subscripts

o	Refers to chamber conditions
i,j	Refer to quantum states
g	Refers to the ground state

SECTION I

INTRODUCTION

The electrodeless discharge operating at high pressure with large power input has been proposed as a means of heating a gas to high enthalpy levels. Such a discharge would find application for high enthalpy aerodynamic testing, solar radiation simulation and to simulate the conditions in a gaseous core nuclear rocket (Ref. 1). Electrodeless discharges offer two potential advantages over the DC arcs traditionally used as gas heaters. First, there are no electrodes in contact with the discharge and electrode contamination is eliminated. Second, there exists an additional independent variable, the discharge frequency, which makes it possible to exercise some control over the spatial distribution of the energy absorbed by the plasma. This provides a means of controlling the maximum temperature of the discharge, for a given power input, thereby providing some control over the radiation from the discharge.

Before large scale facilities can be designed it is necessary to determine proper scaling laws for the discharge. Several analytical studies (Refs. 2, 3 and 4) suggest that the discharge may be scaled by the parameter $r\sqrt{2}\,a/\delta$ where this parameter has a constant value of approximately 2.5. If this were the case the discharge radius would vary inversely with the square root of the discharge frequency. This suggests that larger discharges could be operated at lower frequency. A more recent analysis (Ref. 5) has shown that the scaling does not follow this simple criterion, but that the size of the confining tube exerts a strong influence on the discharge radius. This analysis also shows that for a given power input and confining tube size, the radiation decreases as the discharge frequency is increased.

Another feature of the electrodeless discharge is that it is sensitive to the flow conditions existing in the discharge. Unlike the DC arc the plasma is not attached to electrodes and is, therefore, free to move in response to the fluid flow. Typically the discharge is unsteady and may become unstable in the presence of

even moderate flow velocities. If the discharge is required to operate with large mass flow rates some means must be found to stabilize it. An electrodeless discharge was first stabilized at atmospheric pressure by Reed (Ref. 6) who used a vortex flow in a cylindrical confining tube. This method works well at low flow velocities but will "blow out" when the flow is increased. In the course of this study a more effective means for stabilizing the discharge was discovered. No vortex flow is used but instead, a bluff-body is placed in the entering flow. This produces a recirculation cell in the flow which stabilizes the discharge region. In addition, it has been found that higher bulk temperatures are produced by the discharge when it is stabilized by a bluff body.

The purpose of this study has been to provide accurate experimental data on scaling to check the validity of the theoretical analysis and to study the discharge stability as related to flow. Two discharges were constructed. A small discharge with a confining tube diameter of four inches was operated at a frequency of approximately 4 MHz and pressures from vacuum to approximately two atmospheres. A larger discharge with a confining tube diameter of 7.5 inches was designed to operate at a frequency of approximately 4 KHz and pressures from vacuum to ten atmospheres.

Section II of this report contains a general discussion of the physical processes involved in the inductive electrodeless discharge. Section III describes the experiments performed in the small discharge. Section IV describes the design and initial experiments with the large discharge and Section V contains a summary of the results and conclusions.

SECTION II

DISCUSSION OF THE INDUCTIVE ELECTRODELESS DISCHARGE

2.1 ENERGY PROCESSES

Electrodeless discharges may be classified as either capacitive or inductive. In the capacitive discharge a container of gas is placed between the plates of a capacitor driven by a high-frequency potential. An alternating current flows in a straight path through the gas between the capacitor plates. The current path is completed by displacement currents through the container walls and consequently the currents are generally small. In the usual inductive discharge a cylindrical tube containing the discharge gas is placed within a solenoid coil carrying a high-frequency current. The magnetic field of the solenoid induces closed current rings in the gas. The plasma acts like a short-circuited secondary of a transformer (Ref. 7), and the currents in the plasma may be quite large. For this reason the inductive discharge is preferred for high power applications and the following discussion will apply only to this type of discharge.

The azimuthal electric field induced in the discharge is not uniform but varies with the radial position. In the absence of a discharge the induced electric field decreases linearly to zero on the solenoid axis. In the presence of a plasma the electric field decreases more rapidly as a result of the current rings induced in the plasma. The field penetrates a distance of the order of a skin depth, δ, defined as

$$\delta = \sqrt{\frac{2}{\sigma \mu \omega}} \tag{1}$$

where σ is the plasma conductivity, μ is the permeability and ω is the angular frequency of the applied field. Thus, if δ is small compared to the radius of the discharge, the energy is deposited near the outer surface. For a discharge of a given size some control over the spatial distribution of energy absorption is provided by

controlling the discharge frequency. By decreasing the frequency more energy is absorbed within the column and by increasing the frequency the energy is absorbed nearer the surface.

As a result of this "skin effect" in electrodeless discharges the temperature distribution within the plasma column is considerably different than that of a D.C. arc. Where the peak temperature of a D.C. arc is on the arc axis, the electrodeless discharge has its peak temperature between the discharge axis and the containing wall. The location of this peak can be varied by changing the discharge frequency. Further, for similar discharge powers the value of the peak temperature is considerably smaller for the electrodeless discharge.

The electrical energy absorbed by the discharge is removed from the discharge by several means. Part of the energy is radiated by the plasma, part is conducted through the cooled containing tube and the balance goes into raising the enthalpy of the gas and is subsequently carried away by convection if a flow exists. The equation describing the energy balance is referred to as the Elenbaas-Heller equation and has been studied by several investigators (Refs. 2, 3, 4, 5, 8 and 9). The problem is complicated by the spatial variation in electric field and numerical solutions are usually required. The temperature profiles predicted by the one-dimensional theory exhibit the off-axis peak and are in reasonable agreement with many experiments. However, with the exception of Ref. 5 the effect of flow on the energy balance has been neglected and in certain experiments with strong axial flow (Ref. 10) agreement between theory and experiment is poor. In particular, for the experiment in Ref. 10 strong axial convection reduces the diameter of the discharge below that predicted by the one-dimensional theory.

2.2 STABILITY CONSIDERATIONS

In the electrodeless discharge the plasma column is

not attached to electrodes and is free to be swept out of the exciting coil by a sufficiently high flow velocity. Before a gas may absorb energy from the electric field it must be raised to a temperature where its electrical conductivity becomes significant. If the entering flow is cold it must be heated by conduction, radiation or convection to a temperature at which it is electrically conductive before it passes out of the solenoid region. This process is very similar to that of chemical combustion as pointed out by Raiser (Ref. 11).

For an optically thin plasma radiation is ineffective and thermal conduction is a slow process which is insufficient except for very small flow velocities. Convection, then, must play a dominant role in the heating of the incoming flow. For vortex stabilized discharges the vortex flow induces circulation cells in the tube which convect energy from the hot plasma region back upstream to the colder entering flow. A more direct approach is to induce the circulation cell by means of a bluff-body placed in the entering flow in a manner analogous to a ram-jet combuster. This approach was first utilized in the course of the present study. A complete theoretical analysis of the problem can be found in Ref. 12 where a stability criterion is defined. Basically this criterion requires that the entering flow be heated to some minimum required temperature within a distance less than the length of the circulation cell formed in the wake of the bluff body. As expected intuitively, stability increases with increasing power input and decreasing flow velocity.

Thus, for stability to exist in an electrodeless discharge with flow, it is necessary to establish, by convection or other means, a region, fixed in space upstream of the solenoid, where the flow has been raised to a temperature where the gas is electrically conductive.

SECTION III

EXPERIMENTS WITH A SMALL ELECTRODELESS DISCHARGE

3.1 DESIGN OF THE EXPERIMENT

Previous experience had shown that it was difficult to obtain stable discharges in the presence of large flows. To investigate the behavior of the discharge with various means of introducing the flow a series of experiments were conducted using four-inch diameter containing tubes of various lengths. Several methods of introducing the flow were attempted and evaluated. The first of these was the traditional vortex flow. Next, attempts were made to operate with radial inflow and axial flow. Finally, the bluff-body flow was tried and found to provide a significant improvement in performance. The experiment was designed to provide accurate measurements of flow rate, power input, coil current, bulk temperature and temperature profiles.

To provide accurate measurement of the power input to the discharge, the discharge was excited by a tuned resonant circuit instead of the usual method of operating in a portion of the oscillator circuit. This circuit is shown in Fig. 1. The two ampmeters A_1 and A_2 detect the line current and the circulating current respectively. These signals are fed to a specially designed phase detecting circuit, p , which has zero output when the phase difference between the currents A_1 and A_2 is exactly 90 degrees. At this point the load has a power factor of unity and the power into the load is obtained as the product of the line current A_1 and the line voltage V. The circuit is adjusted by the capacitor C_2 so that a unity power factor is obtained. It was found that the circuit could successfully be adjusted for unity power factor over a wide range of plasma conditions although this does not coincide exactly with the condition for maximum input into the plasma as judged by plasma brightness. The advantage of this technique for power measurement is that it is relatively free of serious measurement errors introduced when measuring power at a point in the circuit where the power factor is small. Further, the harmonic content of the waveform is small at this point

in the circuit in contrast with the situation in the oscillator tank circuit.

The circuit described measures the total power to the tuned circuit. To determine that portion which is lost to components other than the plasma itself, the power into the tuned circuit was measured with no plasma present over a range of circulating currents A_2. The results are shown in Fig. 2. To determine the net power into the plasma the measured power into the tuned circuit was reduced by an amount taken from Fig. 2 at the appropriate value of circulating current.

The individual ampmeters used in the circuit were calibrated against a thermal ampmeter and it is believed that the total error in measured power input into the gas is less than 10 percent.

A bulk temperature was determined for the discharge by utilizing a calibrated orifice at the exit of the discharge. By exhausting through this orifice into a vacuum, sonic flow was insured in the orifice. The mass flow through the discharge was accurately measured using a Wallace-Tiermann flowrater which was calibrated using a Fisher Porter laboratory flowmeter calibration set. Discharge pressure was measured using a common bourdon gauge.

The values of mass flow rate and chamber pressure were measured and having assured sonic flow through the orifice, it was possible to determine the chamber temperature assuming isentropic flow through the orifice. This is the value referred to as bulk temperature and is given by

$$T_o = \left(\frac{P_o A}{\dot{m}}\right)^2 \frac{r}{R} \left(\frac{2}{r+1}\right)^{\frac{r+1}{r-1}} C_d \qquad (2)$$

The term C_d is the discharge coefficient for the orifice

which was determined for each orifice using Eq. 3. for a known bulk temperature (room temperature). The experimentally determined values of C_d for the orifices used in the experiments are given in Table I.

The experiment was designed to provide for a spectroscopic determination of the temperature profile across the radius of the discharge. This measurement is of fundamental importance since this is the quantity which is predicted by the various theories for the discharge.

The emission from an electrodeless discharge is often unsteady and a poor signal to noise ratio makes it difficult to obtain good spectroscopic data. To overcome this problem a signal averaging computer was used together with a rotating mirror to provide repetitive sweeps of the discharge image across the entrance slit of the half-meter ebert monochrometer. A schematic is shown in Fig. 3. A stable trigger signal for the computer was obtained by reflecting a laser beam from the rotating mirror onto a photodiode. With a rotation rate of 112 r.p.m., 64 sweeps could be acquired by the computer in approximately 35 seconds.

In order to obtain the absolute intensity of the radiation from the discharge a tungsten filament lamp, calibrated by Eppley Laboratories, was placed at a location optically similar to that of the discharge. Thus, radiation from the discharge could be compared directly with that from the standard lamp.

The data required for the determination of a temperature profile from the discharge was obtained by the following procedure:

1. The spectrometer was adjusted to the wavelength of the chosen line and the slit set to a bandwidth large compared to the line width.

2. The rotating mirror was started and the computer programmed to acquire 64 sweeps.

3. The spectrometer was adjusted to a new wavelength, near the line, to observe the continuum radiation.

4. The mirror and computer were again started and another 64 sweeps acquired.

5. The mirror was oriented to place the lamp image on the slit and 64 sweeps acquired by the computer.

6. The data acquired in the computer memory was read out onto punched tape for subsequent processing on the IBM 360/65 computer.

In addition to temperature profiles, data was taken on the relative intensity of a number of lines to investigate the state of equilibrium in the discharge. For this measurement the spectral response of the spectrometer was determined using the calibrated tungsten lamp. The spectral response of the spectrometer is shown in Fig. 4.

3.2 STABILITY EXPERIMENTS

A series of experiments were performed with argon using different flow schemes to qualitatively determine the most suitable arrangement. An end plate was made which introduced the flow through 6 nozzles oriented at 45 degrees with the discharge axis to give equal components of axial and tangential velocity to the flow. Discharges using this nozzle plate were operated in tubes of 18 inches and 12 inches of length. It was found that the discharge was very unsteady with mass flows greater than 0.15 gm/sec and that a further increase in flow caused the fluctuations to become unstable and extinguish. It was found that the discharge was more stable in the short tube and the 12 inches long tube was used in all subsequent experiments.

It was thought that bouyancy forces might affect discharge stability and the discharge was inverted so

the flow was vertically downward. This was found to increase the steadiness of the discharge, but only slightly. However, subsequent experiments were all performed with the flow directed vertically downward.

An attempt was made to introduce the flow so that it was directed radially inward toward the discharge axis at a point midway between the ends of the discharge tube. With this flow arrangement the discharge would tend to stay in one of two different modes. In one mode the discharge stayed in the upper half of the discharge tube above the flow inlet. With this arrangement little power was absorbed by the discharge and incoming flow was only slightly heated before leaving the tube through the exit orifice. In the second mode the discharge moved down the tube with equal portions above and below the incoming flow. In this mode a larger amount of power was absorbed by the discharge. Although neither of these modes provided better stability the experiments suggested the existence of recirculation cells in the discharge and the requirement for low flow velocities where the cold flow enters the solenoid coil region.

Since it appeared that a strong recirculation zone aided discharge stability, a bluff body was placed in the entering flow. Strong recirculation cells are established in the wake of such a body. A circular plate, 2 inches in diameter was suspended 2 inches from the upper end plate. The flow was introduced through a simple hole drilled through the upper end plate on the discharge axis.

This configuration was found to be highly effective in stabilizing the discharge. Flow rates five times greater than those obtained with vortex stabilization were easily obtained. Higher flow rates were not attempted since the discharge pressure was now nearly two atmospheres, the safe limit with the Pyrex tubes being used. A further advantage of the bluff body stabilized discharge was also noted. With vortex stabilization it was often difficult to make the transition from a low pressure to a high pressure discharge. The flow had to

be increased very slowly or the discharge would become unstable and extinguish. With the bluff body stabilization this transition could be made as rapidly as desired with no indication of instability.

It was found, however, that when very small exit orifices were used the discharge would not make the transition from low to high pressure at all. It is thought that in this case the flow velocities are too small to establish the required recirculation in the wake of the bluff body. At the small flow rates where this was observed the Reynolds number was approximately 10, the value at which transition to separated flow first begins.

To illustrate the formation of the recirculation cell in the wake of the bluff body a water flow experiment was performed. A two inch aluminum disk was suspended in one of the discharge tubes and a tank of water mounted above it. The water was allowed to flow downward by opening an exit valve at the bottom. The flow rate was adjusted to have a Reynolds number of 200, approximately that of the discharge, and the flow was photographed using milk for flow visualization. A photograph of the circulation cell formed is shown in Fig. 5.

3.3 DETAILED EXPERIMENTS

Once the stable bluff body configuration was found experiments were performed to measure temperature profiles for this discharge. In addition, a number of experiments were performed to determine the variation of bulk temperature as a function of flow rate and power input. For comparison, several similar experiments were performed using vortex stabilization.

The temperature was determined by measuring the absolute intensity of the 4158 Å line of atomic argon. This method is relatively insensitive to measurement errors and the transition probability has been determined to good accuracy (Ref. 13). The value due to Gericke was used in data reduction. The use of the absolute intensity method requires the assumption that the plasma

is in local thermodynamic equilibrium (LTE) for a determination of temperature. The emission coefficient is given by

$$\mathcal{E} = \frac{h\nu}{4\pi} A_{ij} N_i \tag{3}$$

If the plasma is in LTE the number density of atoms in the upper excited state, N_j, can be related to the number density in the ground state by the relation

$$N_i = N_g \frac{g_i}{Z} e^{-\epsilon_i/kT} \tag{4}$$

The emission coefficient is given in terms of ground state number density and the electron temperature as

$$\mathcal{E} = \frac{hc}{4\pi\lambda} A_{ij} N_g \frac{g_i}{Z} e^{-\epsilon_i/kT} \tag{5}$$

The number density in the ground state at various temperatures and pressures is given for argon in Ref. 14 while the statistical weight and transition probability were taken from Ref. 13. Equation 5 can be solved giving a relationship for the temperature as a function of the emission coefficient and ground state number density. A plot of this function is given in Fig. 6 for argon at a pressure of one atmosphere.

Emission coefficients were obtained for a discharge by inverting radial scans of the discharge as outlined in Section 3.1 and performing an Abel inversion of the data with the aid of an IBM 360/65 computer. The emission coefficients obtained from the inversion were converted to a temperature profile with the aid of Fig. 6.

A typical bluff body stabilized discharge for which temperature profiles were obtained is shown in Fig. 7.

A similar discharge with vortex stabilization is shown in Fig. 8. A measured emission coefficient profile is shown in Fig. 9. The corresponding temperature profile is given in Fig. 10. The discharge conditions for which this temperature profile was taken are:

Frequency - 4 MHz
Gas - Argon
Tube Size - 12 inches long, 4 inches diameter
Bluff Body - 2 inches diameter disk transverse to flow
Coil - 5 1/2 turns of 1/4 inch diameter copper tubing
9 1/2 inches mean diameter, 6 inches long
Pressure - 1 atmosphere
Mass Flow - 0.202 gm/sec
Exit Orifice - 0.059 inches diameter
Circulating Current - 30 amps (rms)
Total Input Power - 2.10 KW
Net Input Power - 1.75 KW
Generator Plate Power - 7.59 KW
Bulk Temperature - 1487°K

Also shown in Fig. 10 is a temperature profile obtained in a similar discharge except vortex stabilized, and a theoretical temperature profile obtained from the method of Ref. 5. The detailed parameters for the vortex discharge were not recorded.

The temperature profiles of Fig. 10 show that the bluff body produces a more uniform temperature profile than the vortex. This is believed to be due to the stronger convective transport of energy toward the discharge axis by the strong circulation in the wake of the bluff body. The theory predicts a peak temperature 4.4% greater than that measured, and the maximum occurs at a much greater radius. This occurs since the theory does not account for the energy convected into the discharge by recirculation or the energy lost downstream by axial convection.

If the plasma is in LTE and the emission coefficients of a number of different lines of wavelength λ

are measured, the quantity

$$B_\lambda = \log\left(\frac{\varepsilon\lambda}{A_{ij}g_i}\right) = -\frac{\epsilon_i}{kT} \qquad (6)$$

The quantity B_λ should produce a straight line whose slope is inversely proportional to the temperature when plotted as a function of ϵ_i .

A number of lines were chosen from Ref. 13 for which Gericke had given transition probabilities. The intensities of these lines were measured and the result is shown in Fig. 11 where it has been assumed that the emission coefficient is proportional to the intensity. For comparison, the straight line is shown which corresponds to the temperature determined by the absolute intensity method. The discrepancy from the expected result is apparent. This experiment was performed on several different discharges with essentially the same results.

To check the validity of the assumption that the emission coefficient is proportional to intensity three lines, 4158 Å, 5558 Å and 6095 Å, were chosen and radial profiles obtained. These were Abel inverted and the resulting emission coefficients for the three lines are shown in Fig. 12. The quantity B_λ was plotted as a function of ϵ_i for three radial locations. The results, shown in Figs. 13, 14 and 15, are similar to those for which it was assumed that the emission coefficient was proportional to the intensity.

The experiments described above have failed to verify the existence of LTE in the discharge. Thus, the temperature determined by the absolute intensity method is open to question.

A series of experiments was performed with a bluff body stabilized discharge operated at a pressure of one atmosphere of argon to determine the effects of flow rate

and input power on the bulk temperature. Exit orifices of several sizes were used to provide a reasonable range of mass flow rates. Three experiments were also performed for the vortex stabilized discharge in order to provide a comparison. The results are presented in Table 2.

An important advantage of the bluff body stabilized discharge is immediately apparent from the data shown in Table 2. In all cases the flow rates are greater for the bluff body discharge than for the vortex discharge. This is especially significant since the largest flow rate shown for the vortex discharge represents the largest flow rate for which stability was obtained. However, the largest flow rate shown for the bluff body does not represent the highest possible flow rate but represents a limit imposed by the exit orifice diameter. For this series of experiments the maximum flow rate for the bluff body is 3.85 times greater than that for the vortex discharge.

In Fig. 16 the input power for the discharge has been plotted as a function of the flow rate. The negative slope for a given exit orifice diameter occurs because as the mass flow was increased the input power had to be decreased in order to maintain the discharge at a constant pressure of one atmosphere. The general trend of the data shows that increased mass flow must be accompanied by increased power input, as expected.

In Fig. 17 the enthalpy, based on the bulk temperature, is shown as a function of input power. The entahlpy is approximately a linear function of the input power, independent of the exit orifice diameter. The maximum enthalpy obtained with the bluff body is 3.3 times greater than that obtained with vortex stabilization. Thus, for the bluff body both enthalpy and mass flow are significantly increased.

A heating efficiency for the discharge can be defined as the fraction of the input power which is carried away by the exhaust flow. The power carried away by the exhaust flow is the product of the enthalpy and the mass flow rate.

Thus,

$$\text{heating efficiency} = \frac{\text{enthalpy x mass flow rate}}{\text{input power}}$$

The heating efficiency has been plotted as a function of the input power (Fig. 18) and the mass flow rate (Fig. 19). The heating efficiency has an approximately linear increase with input power with the maximum efficiency for the bluff body 10 times that of the vortex. The data of Fig. 19 suggest that, for a given orifice size, the heating efficiency passes through a minimum as the flow rate is increased. Beyond this minimum the heating efficiency increases even though the power input is decreased.

This indicates that better mixing of the mainstream with the hot plasma core occurs as the velocity is increased, a result which is supported by the general trend of the data of Fig. 19.

SECTION IV

EXPERIMENTS WITH LARGE ELECTRODELESS DISCHARGES

A large discharge was constructed, similar to the 4-inch vortex discharge, scaled so the parameter $r_2 a/\delta$ was constant. The tube diameter was 12 inches and the frequency was 350 KHz . The electrical circuit was similar to that for the smaller discharge except that tuning was accomplished by varying the length of the work coil.

Discharges were easily initiated in both argon and nitrogen at pressures below 1 Torr. A photograph of a typical low pressure discharge is shown in Fig. 20. As the flow and pressure were increased the discharge took on the familiar oblate spheroid shape and when the flow was increased further the discharge became unstable and extinguished. Detailed measurements were not obtained for this discharge, but the power input was 20-40 KW at pressures below 1/3 atmosphere. On one occasion the flow was increased in an argon discharge until atmospheric pressure was reached. The discharge was highly unsteady and confined to a narrow column which twisted and spiralled around the tube. At one atmosphere pressure this discharge absorbed 110 KW. Experiments with the 12-inch diameter tube were discontinued and a new chamber was designed which would permit continuous operation at pressures to 10 atmospheres.

The high pressure discharge chamber was designed with a thin quartz tube, 7.5 inches in diameter, for the containing tube. A water cooled bluff body was provided for stabilization. A photograph of the tube and bluff body is shown in Fig. 21. A fiberglass tank surrounds the quartz tube and water at high pressure flows in the annulus between the cylinders cooling the discharge and balancing the pressure forces on the inner quartz tube. The fiberglass pressure vessel and associated cooling system is shown in Fig. 22. The heated cooling water which leaves the discharge chamber passes through a heat exchanger and a circulating pump to a pressure balance tank. In this tank the water pressure is adjusted

to chamber pressure through a thin diaphragm. The diaphragm pressure is controlled by a static pressure tap into the discharge chamber. The system is represented schematically in Fig. 23.

This discharge was designed to operate directly in a portion of the power oscillator tank circuit to provide a more efficient power transfer. This caused some difficulties in discharge initiation since the voltage drop across the work coil was small.

The first attempt to initiate a discharge in the high pressure chamber failed when the quartz tube fractured during vacuum pump-down. It was determined that the failure occured as a result of non-uniform axial loading of the quartz tube by the end flanges.

When the chamber was modified and a new quartz tube obtained it was found that the discharge would not initiate from the fields produced by the work coil, even at a current of 1500 amperes. The discharge chamber was modified to provide electrical isolation of the two aluminum end flanges and the discharge was initiated by connecting the upper end flange to the work coil through a small inductor. Low pressure argon discharges of 1-3 sec. duration were initiated several times using this technique. During an attempt to operate for a longer duration, the quartz tube fractured after approximately 10 sec. of operation. The DC plate power during this run rose from 35 KW to 160 KW before the quartz failed.

Subsequent examination of the discharge chamber showed that arcs, produced by the direct excitation of the end flange, had attached to the end flange at a point where the quartz tube was subject to a high mechanical stress produced by the sealing "O" ring. The combination of high mechanical and thermal stress was believed to be responsible for the failure.

The discharge chamber was further modified and a new quartz tube obtained, but no further experiments were possible within the allotted time.

SECTION V

SUMMARY AND CONCLUSIONS

It was discovered, during the course of this study, that the stability of an electrodeless discharge is greatly improved by the use of a bluff body in the entering flow. At comparable pressure and power input a three-fold increase in flow rate was readily attained. Spectroscopic measurements and water flow studies show that the stability is improved as a result of the circulation cell formed in the wake of the bluff body. Measurements of the bulk temperature indicate an order of magnitude improvement in the heating efficiency of the device when bluff body stabilization is used. Further, for the small power levels involved in this experiment, the heating efficiency increases with increasing power input and flow rate. It is significant that the data show no tendency for the heating efficiency to level out, with increasing power input and flow rate, for the range of powers studied. The maximum heating efficiency of 18% reported would appear to have been limited only by generator and circuit limitations.

A large, high pressure discharge chamber was constructed. Due to structural failure of the quartz tubes and the limitations of time, only limited, preliminary information was obtained from this facility.

Electrodeless discharges have been proposed for applications as both gas heaters and light sources. It can be concluded that for applications as a gas heater the bluff body stabilized discharge is superior. However, for light sources, the small fraction of energy absorbed by the flow is an advantage, and vortex stabilization is indicated. The data obtained from this study indicate an increasing heating efficiency with discharge power. Further experiments are needed to determine the limit of this trend. A considerable extension of the range of data should be possible in the high power facility which was constructed.

The markedly different performance of the vortex and bluff body stabilized discharges suggest that further

analytical studies of the electrodeless discharge should be undertaken. Present theories can not distinguish between these two discharges and account must be taken of the axial convection in any successful theory of the electrodeless discharge.

REFERENCES

1. Ragsdale, R. G., "Status of Open-Cycle Gas-Core Reactor Project Through 1970." NASA TM X-2259, March 1971.

2. Hollister, D. D., "An Investigation of the High Pressure Electrodeless Arc In Air," AFFDL-TR-68-160, February 1969.

3. Soshnikov, V. N. and Trekhov, E. S., "The Theory of High-Frequency Vortex Discharges at High Pressure. I" High Temperature, Vol. 4, pp. 165-171, 1968.

4. Soshnikov, V. N. and Trekhov, E. S., "On the Theory of the High-Frequency Turbulent Discharge at High Pressure. II" High Temperature, Vol. 4, pp. 318-321, 1967.

5. Keefer, D. R., Sprouse, J. A. and Loper, F. C., "The Confined Electrodeless Arc," Bulletin of the American Physical Society, Ser. II. Vol. 15, No. 3 pp 413, March 1970.

6. Reed, T. B., "The Induction Coupled Plasma Torch." J. Appl. Phys., Vol. 32, 821-824, 1961.

7. Sprouse, J. A., "Solenoids Excited at Radio-Frequencies in the Presence of Plasmas." AEDC-TR-70-206 October, 1970.

8. Eckert, H. U., "Analytical Treatment of Radiation and Conduction Losses in Thermal Induction Plasmas" SAMSO-TR-69-386, November 1969.

9. Pridmore-Brown, D. C., "A Numerical Study of the Inductive Electrodeless Discharge" SAMSO-TR-70-12, November 1969.

10. Roman, W. C., "Experimental Investigation of a High-Intensity R-F Radiant Energy Source to Simulate the Thermal Environment in a Nuclear Light Bulb Engine" United Aircraft Research Laboratories Report J-910900-4, September (1970).

11. Raiser, Yu P., "High Frequency Discharges in a Gas Flow as a Process of Slow Burning," Aerospace Corporation, LRG-69-T-6, April 1969.

12. Martin, R. E., "Aerodynamic Stability In An Electrodeless Arc," Master's Thesis, University of Florida, December 1970.

13. Adcock, B. D. and Plumtree, W. E. G., "On Excitation Temperature Measurements in a Plasma-Jet, and Transition Probabilities for Argon Lines" J. Quant. Spectrosc. Radiat. Transfer, Vol. 4 pp. 29-39, 1964.

14. Drellishak, K. S., Knopp, D. F., and Cambel, A. B., Partition Functions and Thermodynamic Properties of Argon Plasma," AEDC-TDR-63-146, August 1963.

APPENDICES

I. TABLES

II. ILLUSTRATIONS

Table I

Orifice Diameter (inches)	Discharge Coefficient C_d
0.046	0.77
0.052	0.71
0.059	0.72
0.059	0.67
0.073	0.70
0.100	

TABLE 2

Type Stabilization	Mass Flow Rate (gm/sec)	Power Input (KW)	Bulk Gas Temperature (^{o}K)	Enthalpy (cal/gm.)	Heating Efficiency%
Vortex	0.075	1.98	1190	147	1.75
	0.104	1.75	560	69	0.80
	0.120	1.62	460	57	0.61
Bluff Body	*0.202	1.75	1487	184	7.1
	0.228	1.58	1166	145	6.5
	0.241	3.04	2190	272	7.8
	0.277	2.49	1660	206	7.9
	0.306	2.08	1360	169	8.1
	0.319	1.77	1240	154	8.9
	0.345	3.57	3920	486	18.1
	0.391	3.30	3060	380	16.9
	0.404	3.14	2870	356	16.8
	0.433	2.88	2490	309	17.1
	0.462	2.60	2180	270	17.4

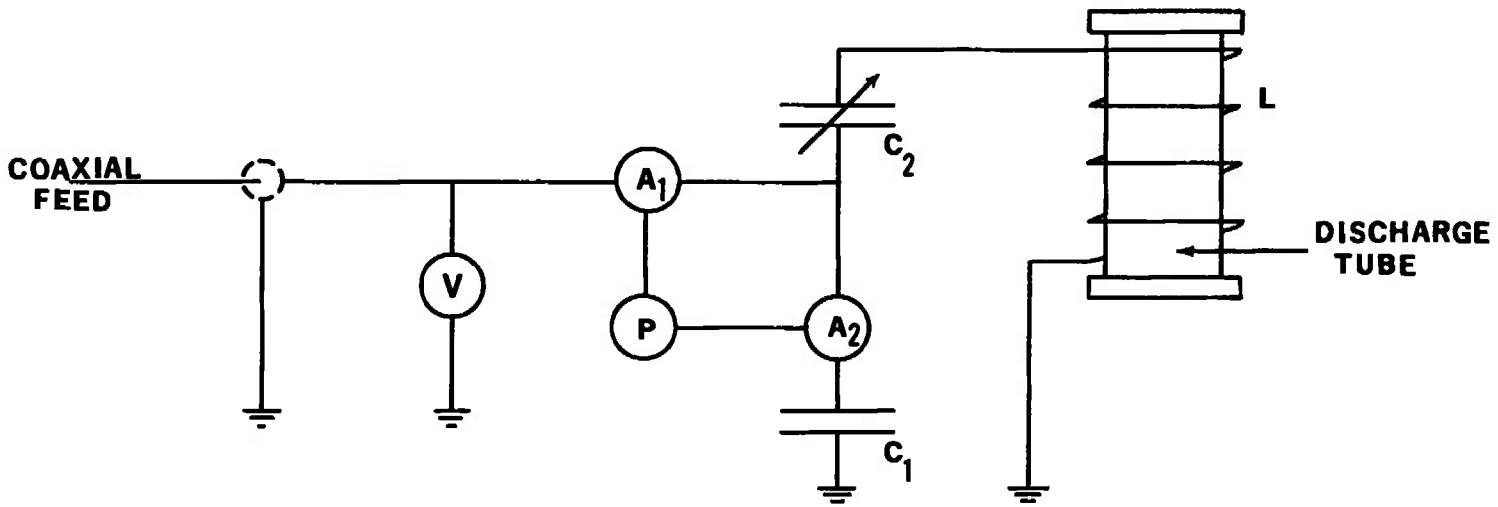

Fig. 1 Schematic of the electrical circuit used to excite the discharge.

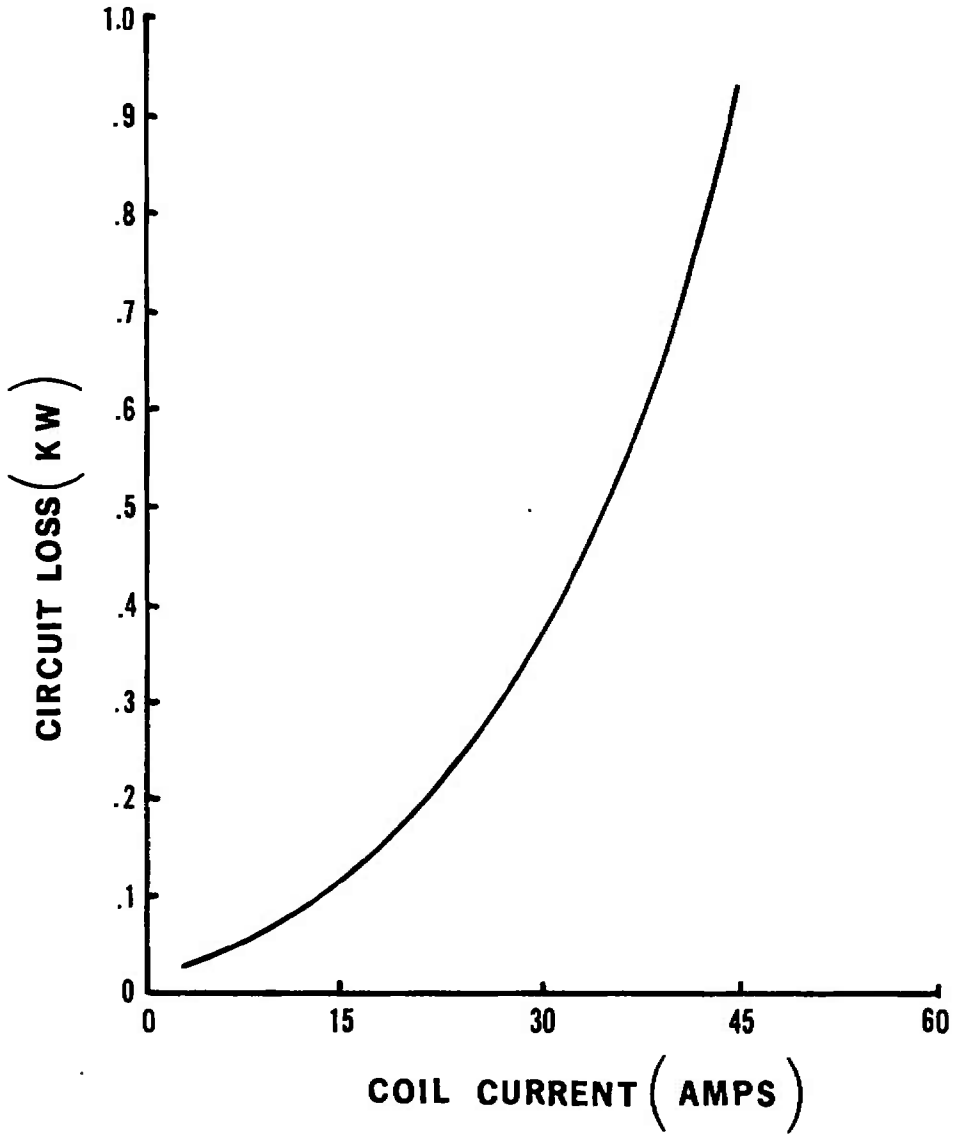

Fig. 2. Circuit losses as a function of the circulating current.

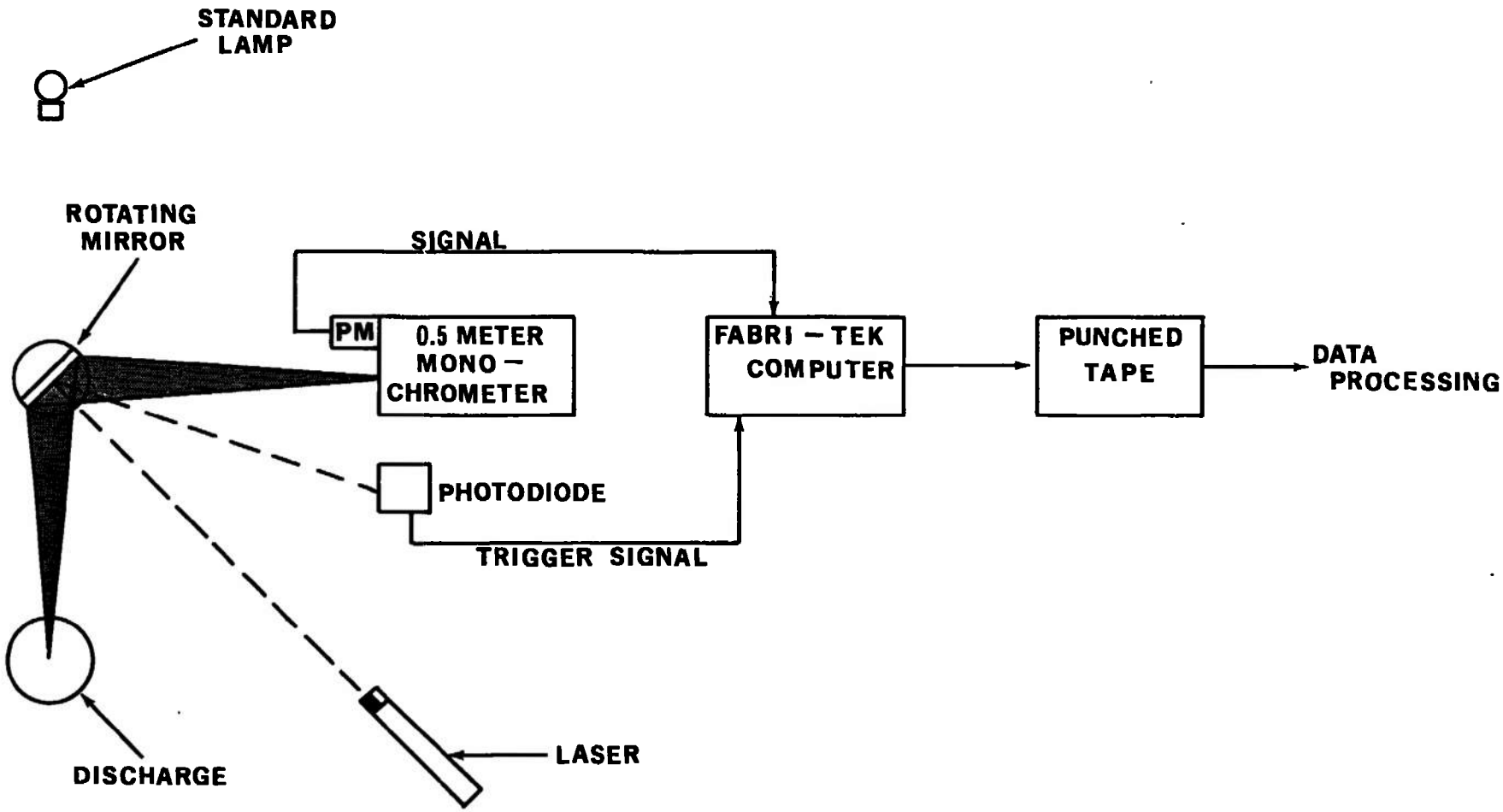

Fig. 3. Schematic of the spectroscopic measuring system.

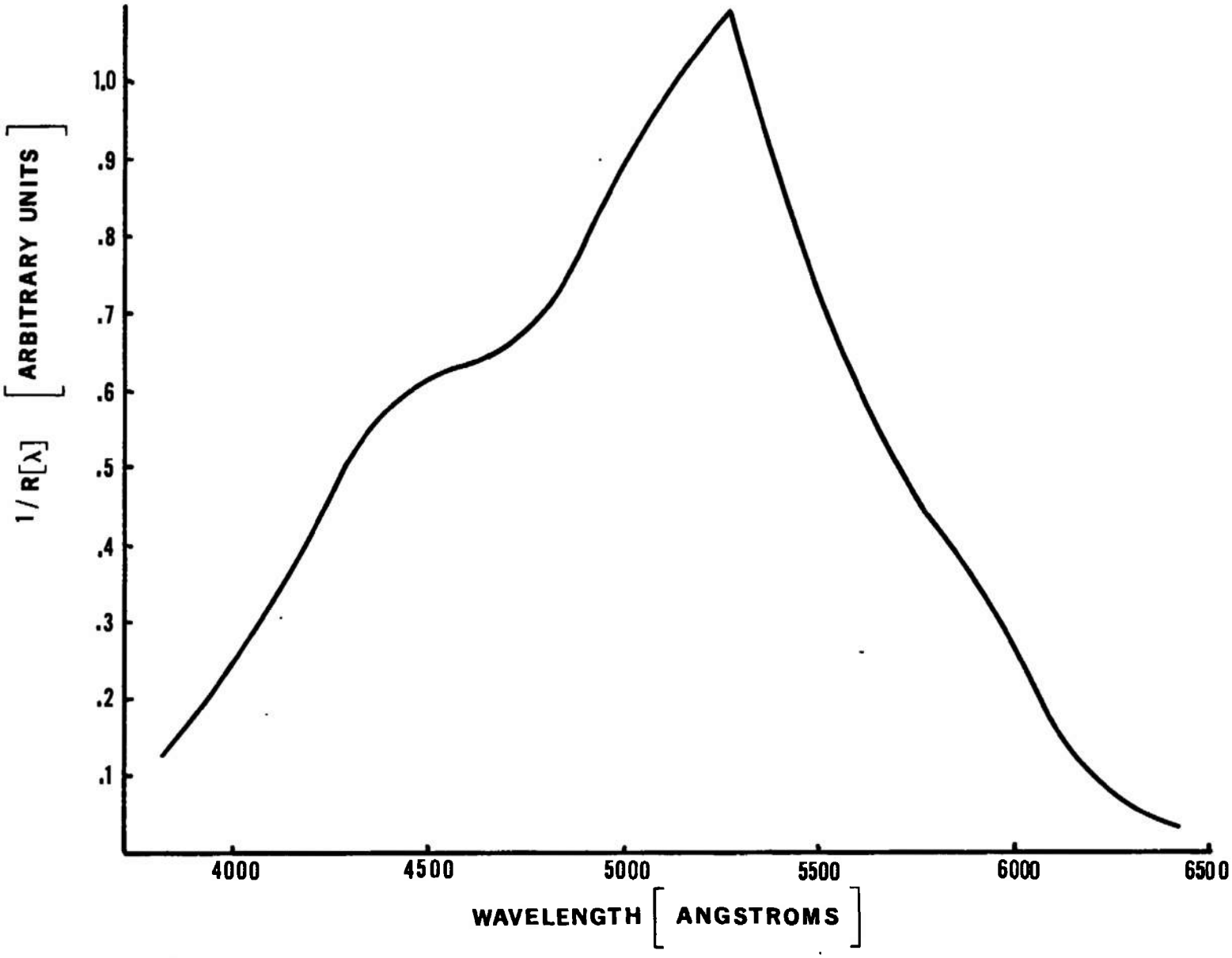

Fig. 4. Spectral response curve for the 0.5 meter spectrometer.

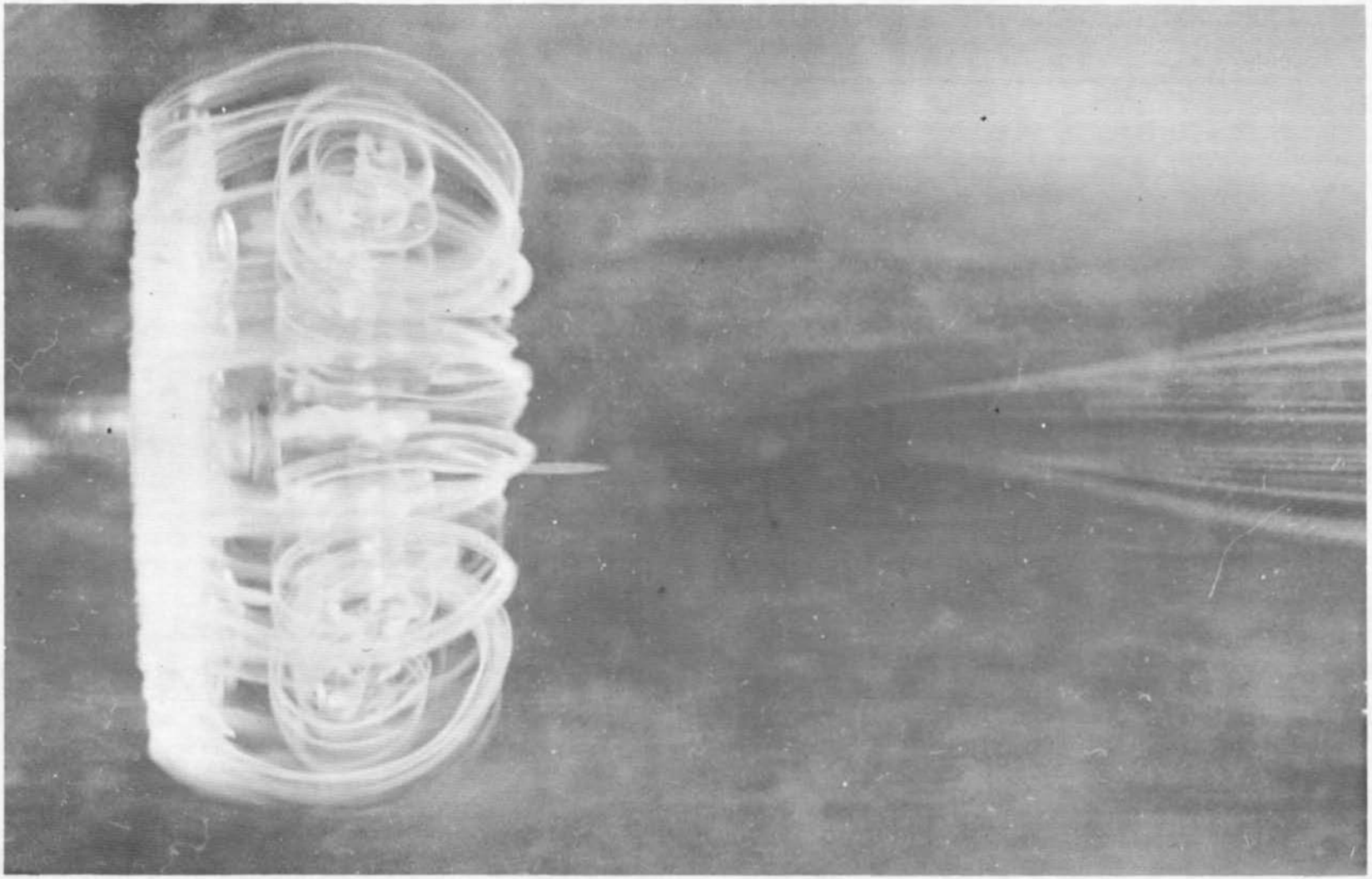

Fig. 5. Water flow visualization of the circulation cell in the wake of the bluff body.

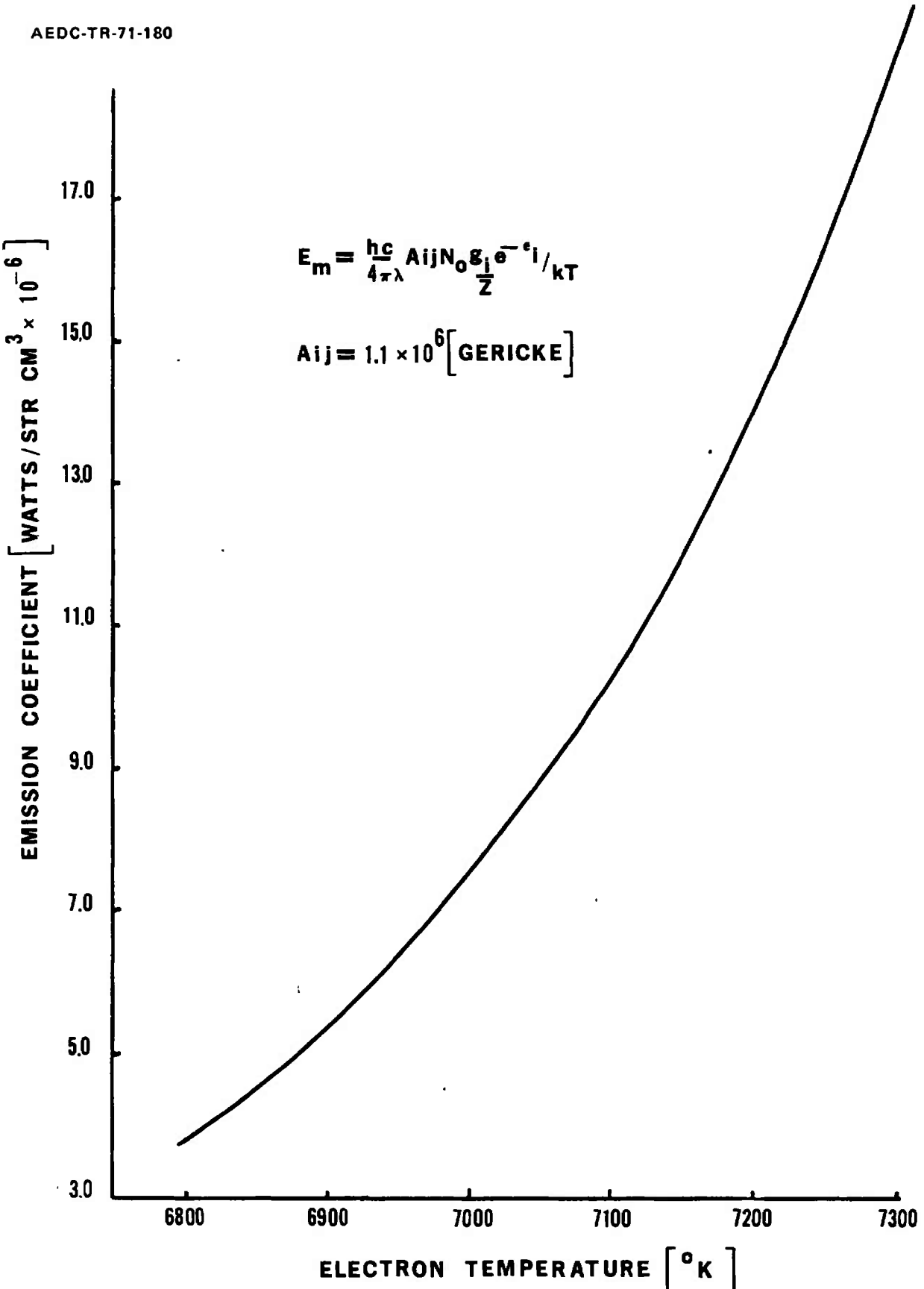

Fig. 6. Emission coefficient for the 4158 Å line in argon at a pressure of 1 atmosphere

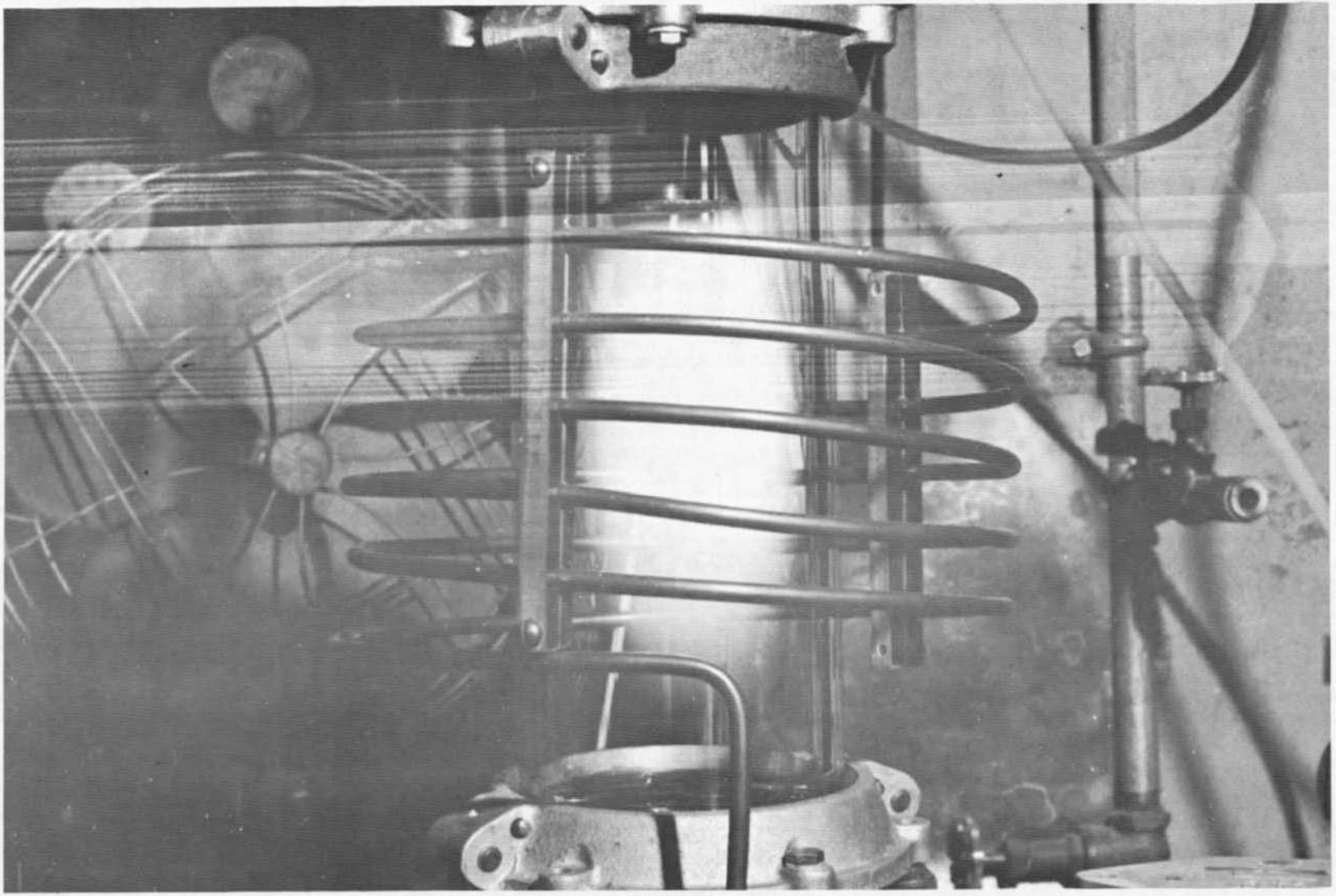

Fig. 7. Typical bluff body stabilized discharge.

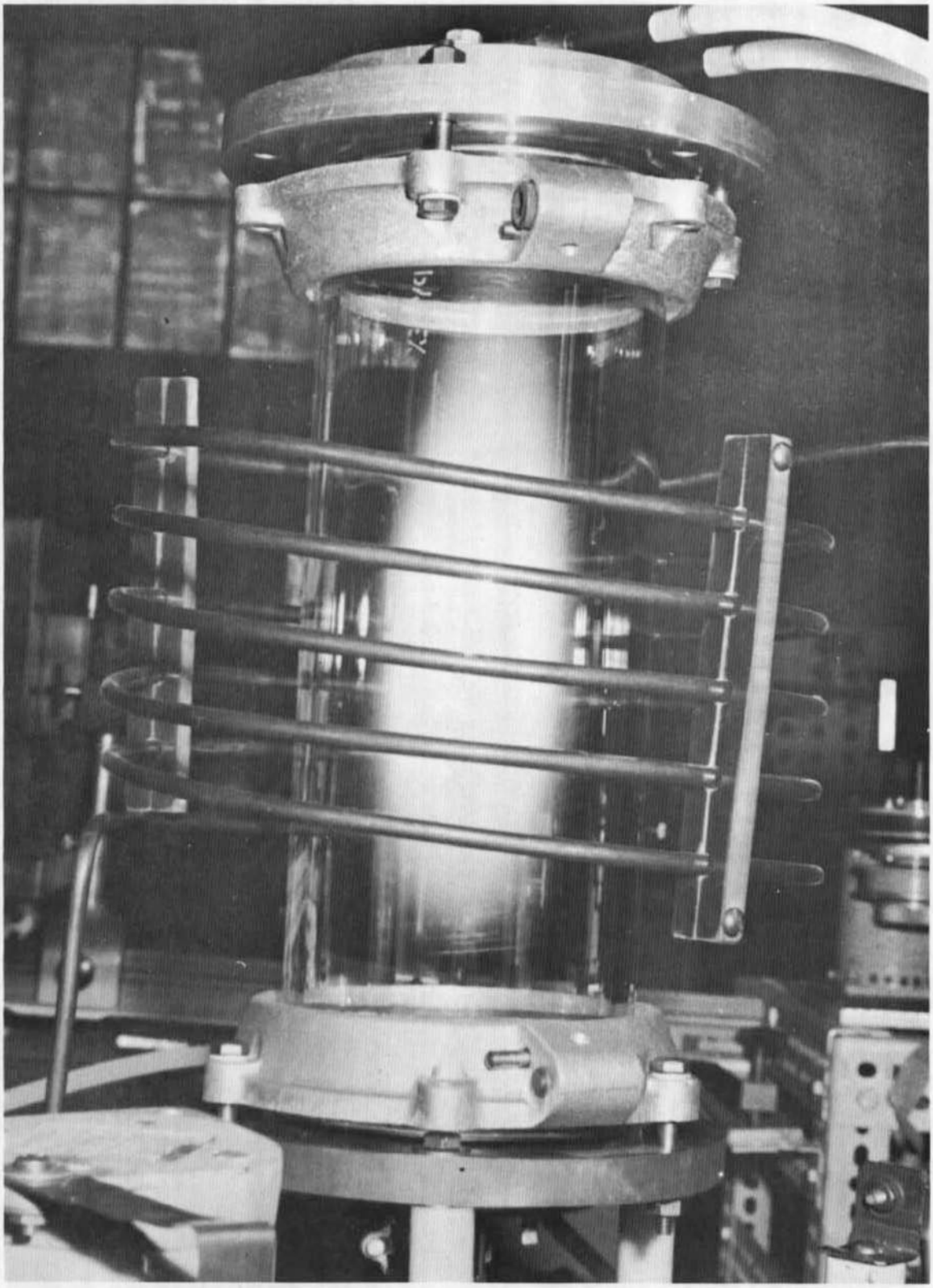

Fig. 8. Typical vortex stabilized discharge.

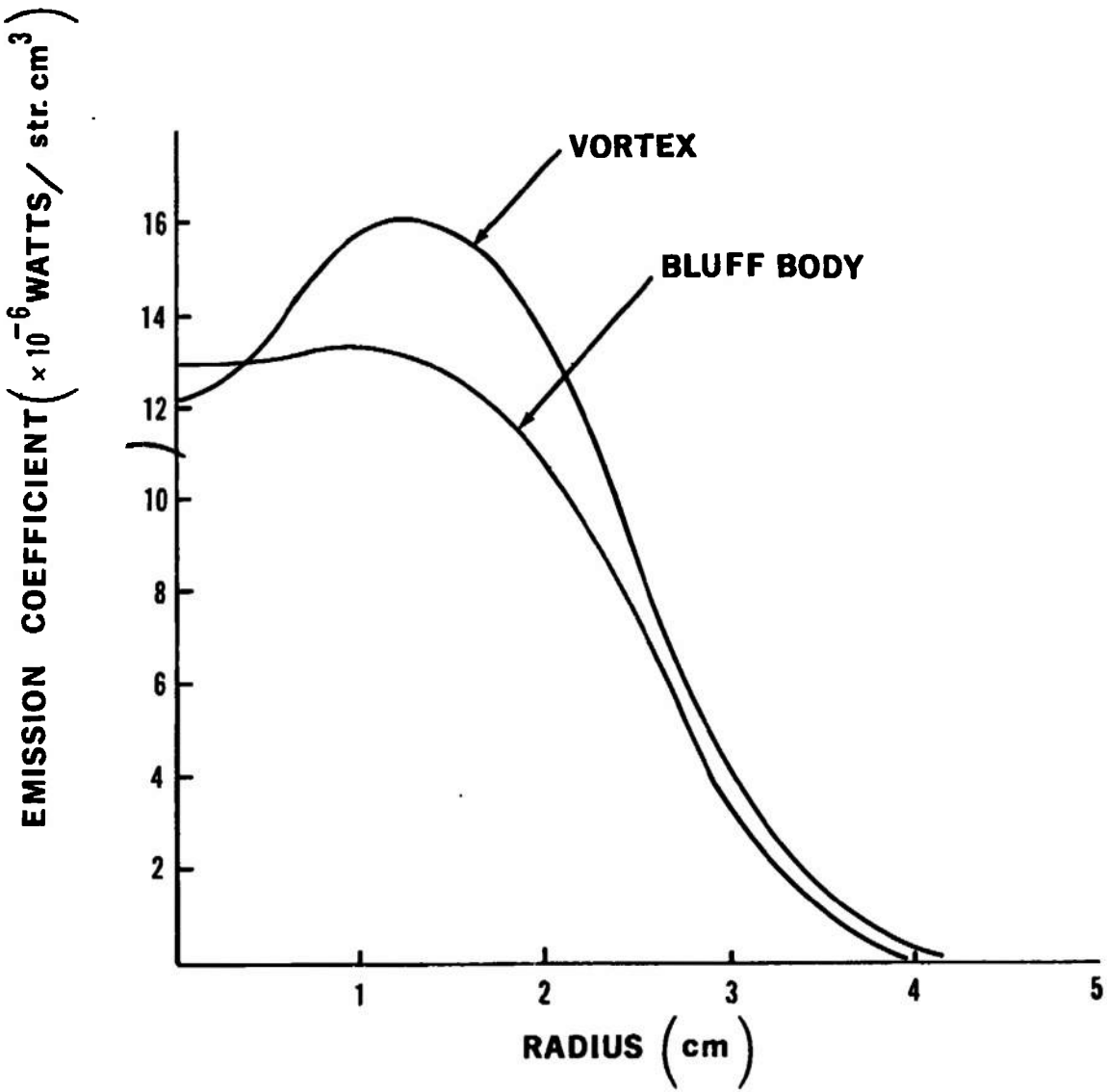

Fig. 9. Emission coefficients for the 4158 Å line.

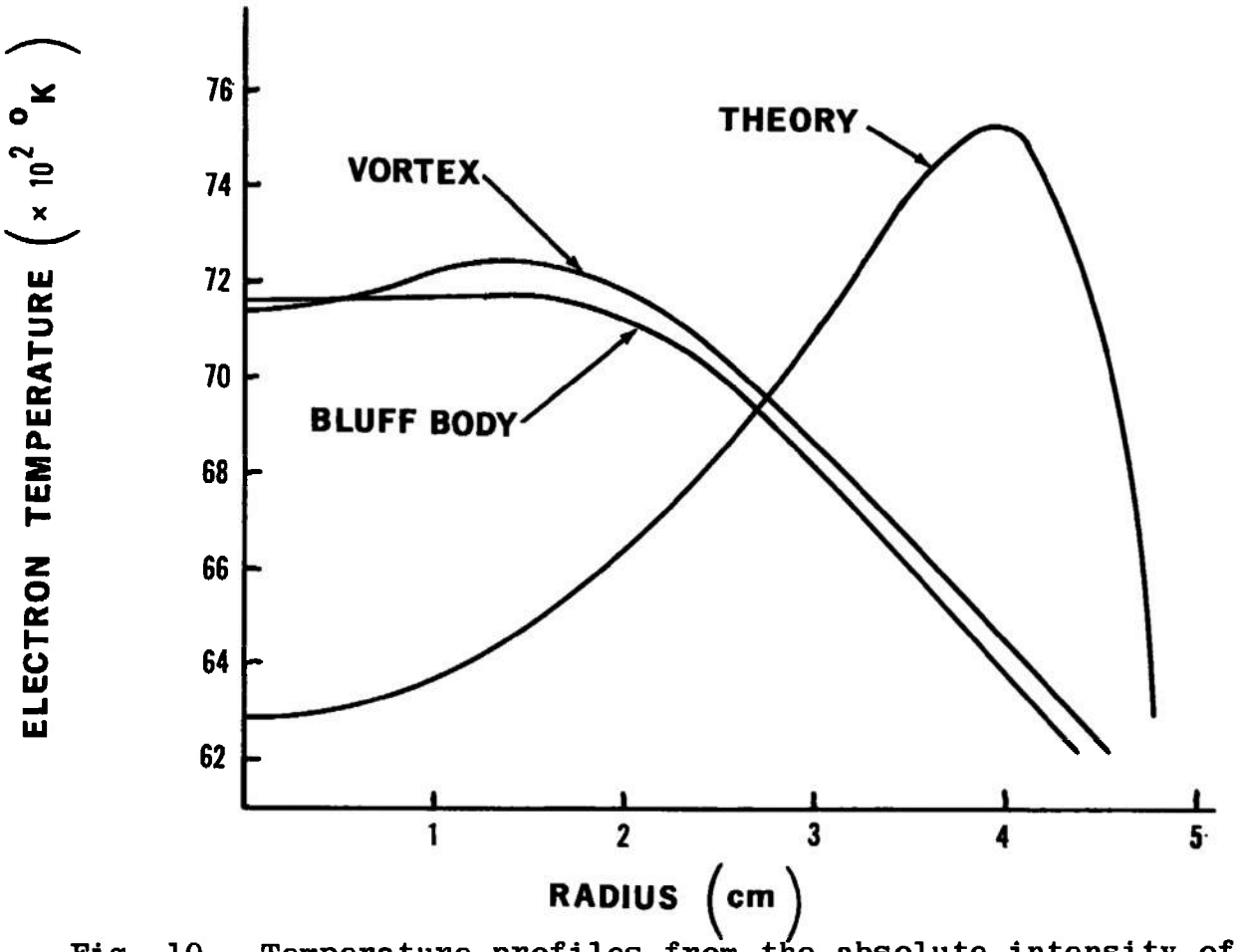

Fig. 10. Temperature profiles from the absolute intensity of the 4158 Å line compared to theory (Ref. 5).

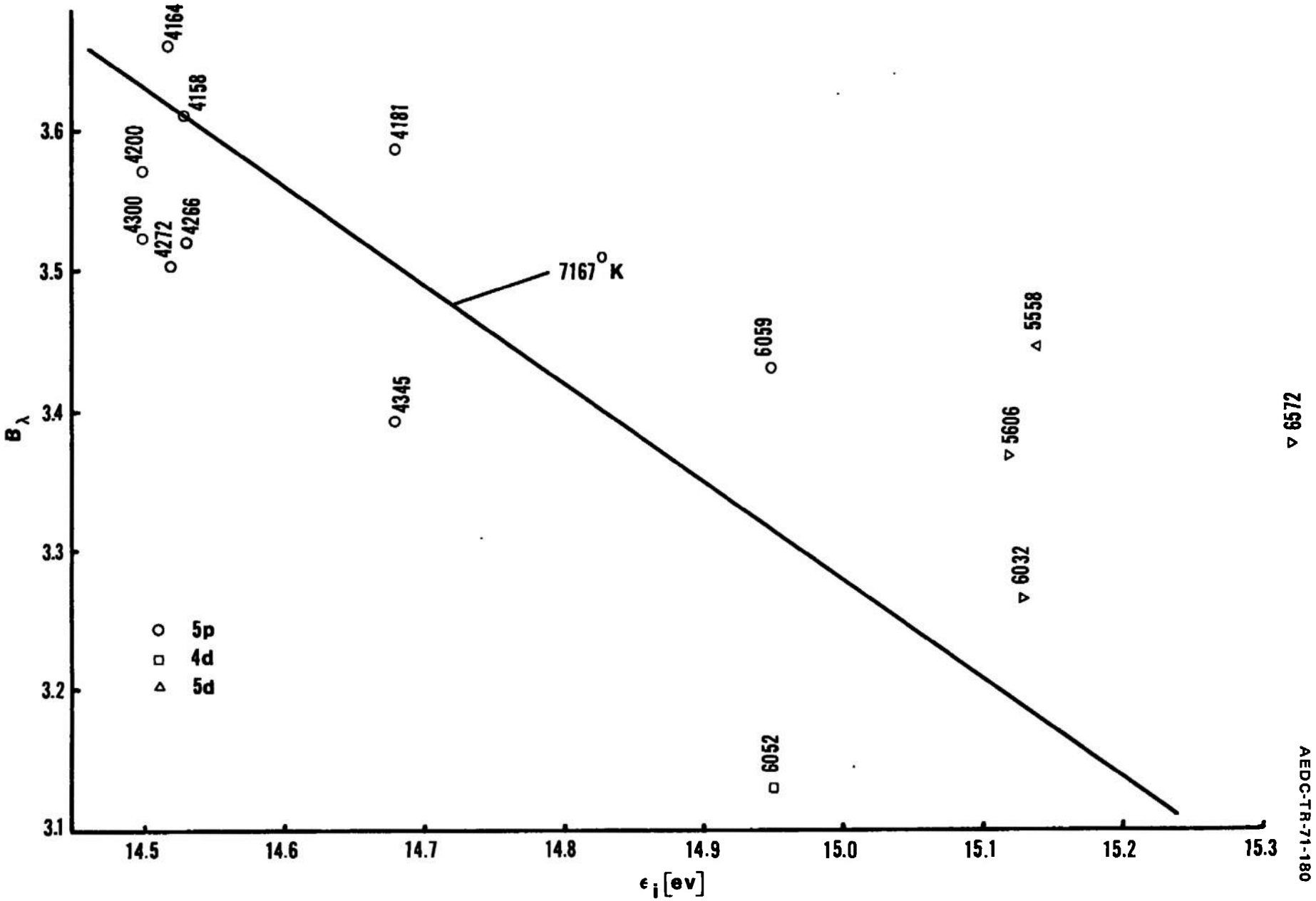

Fig. 11. Boltzmann plot for several argon lines.

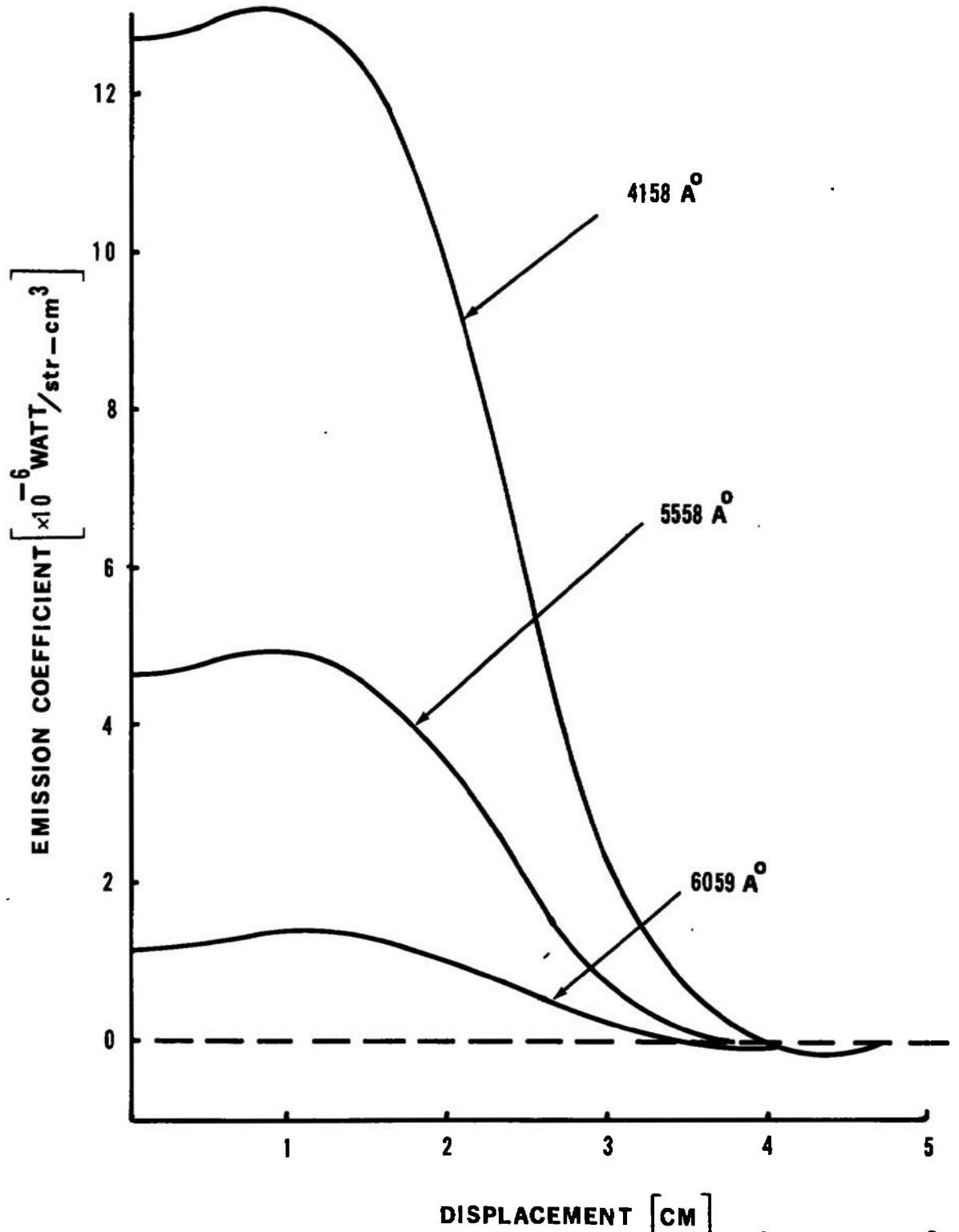

Fig. 12. Emission coefficients for 4158 Å, 5558 Å and 6059 Å.

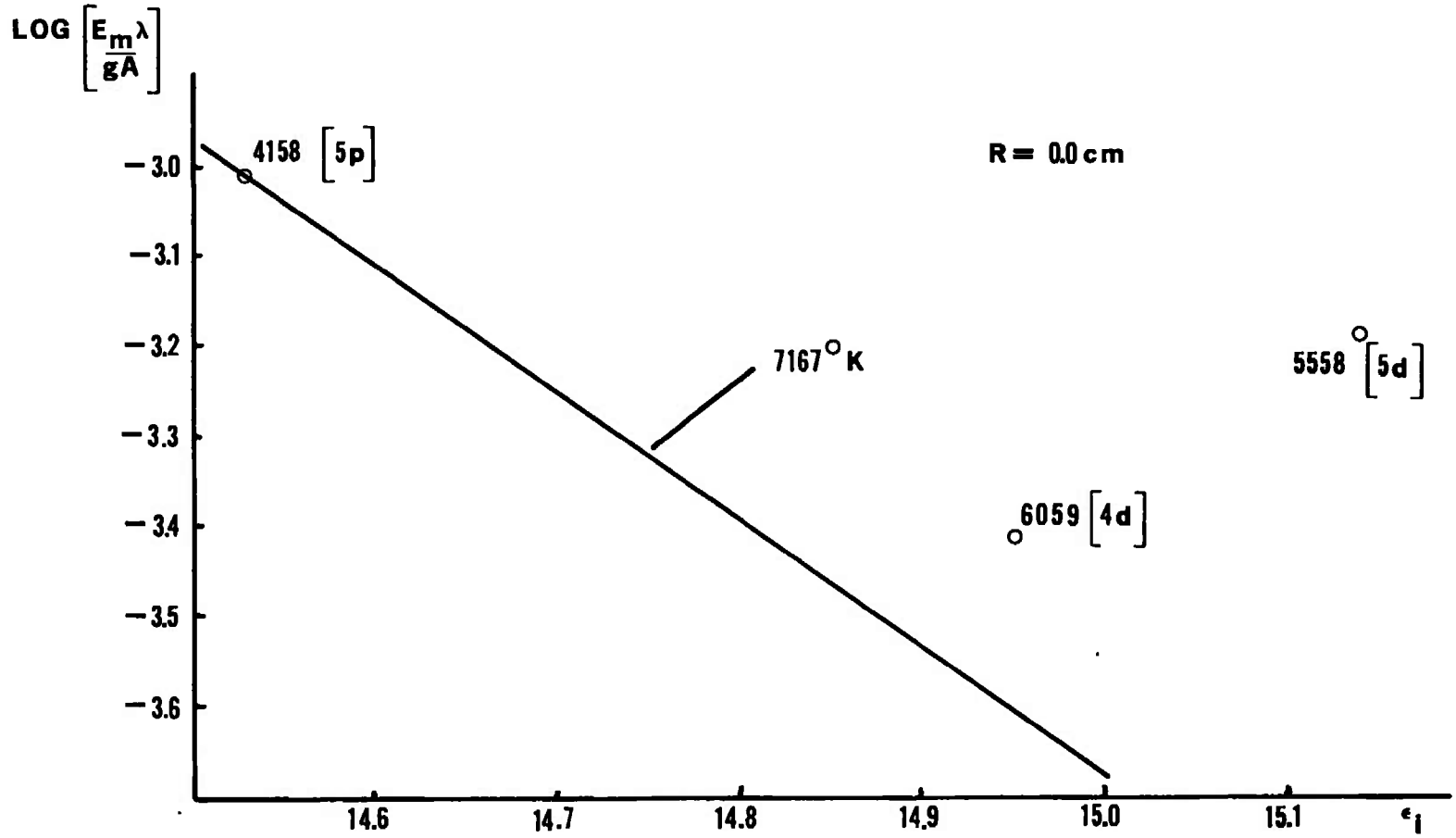

Fig. 13. Boltzmann plot at the discharge axis.

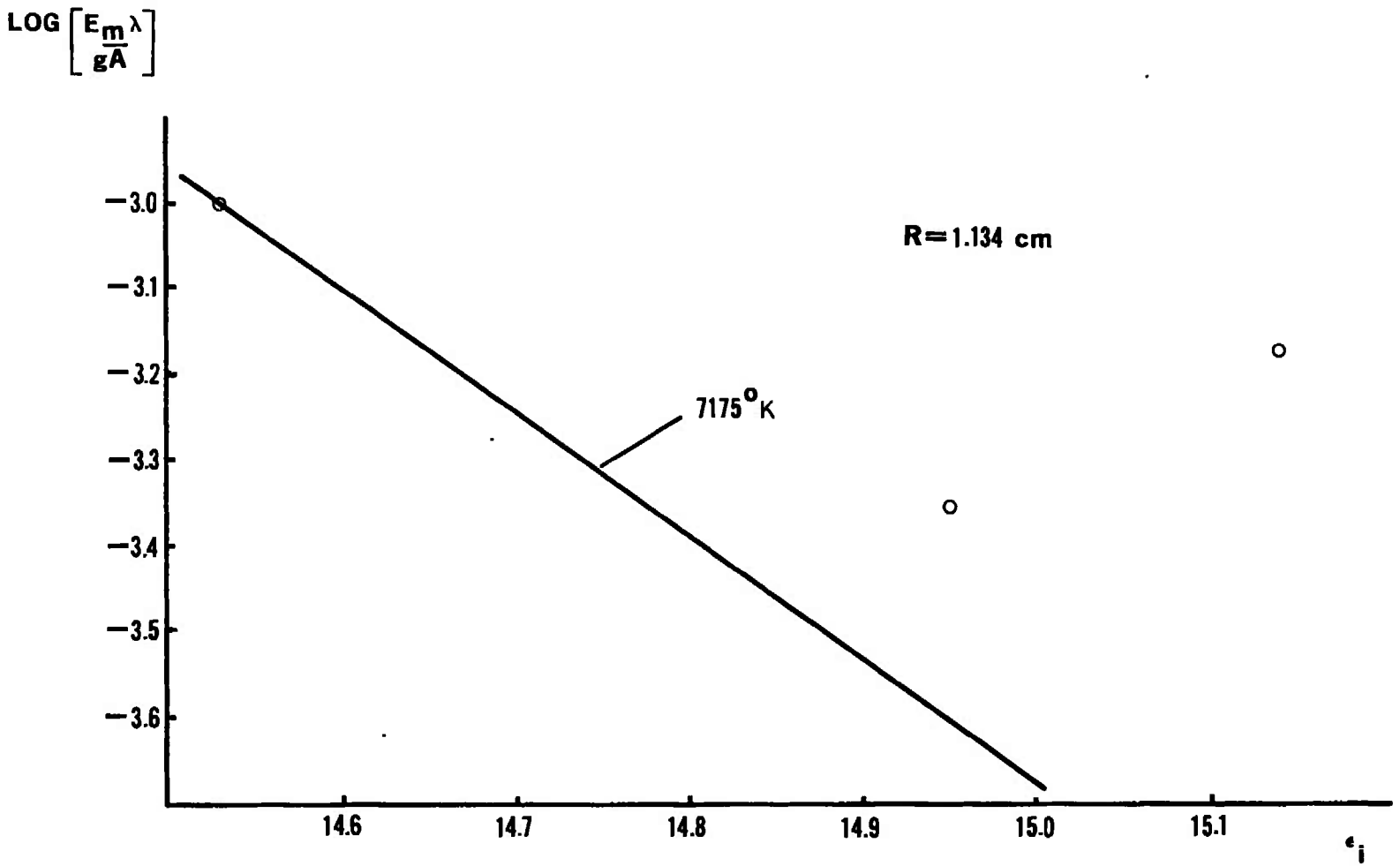

Fig. 14. Boltzmann plot at a radius of 1.134 cm.

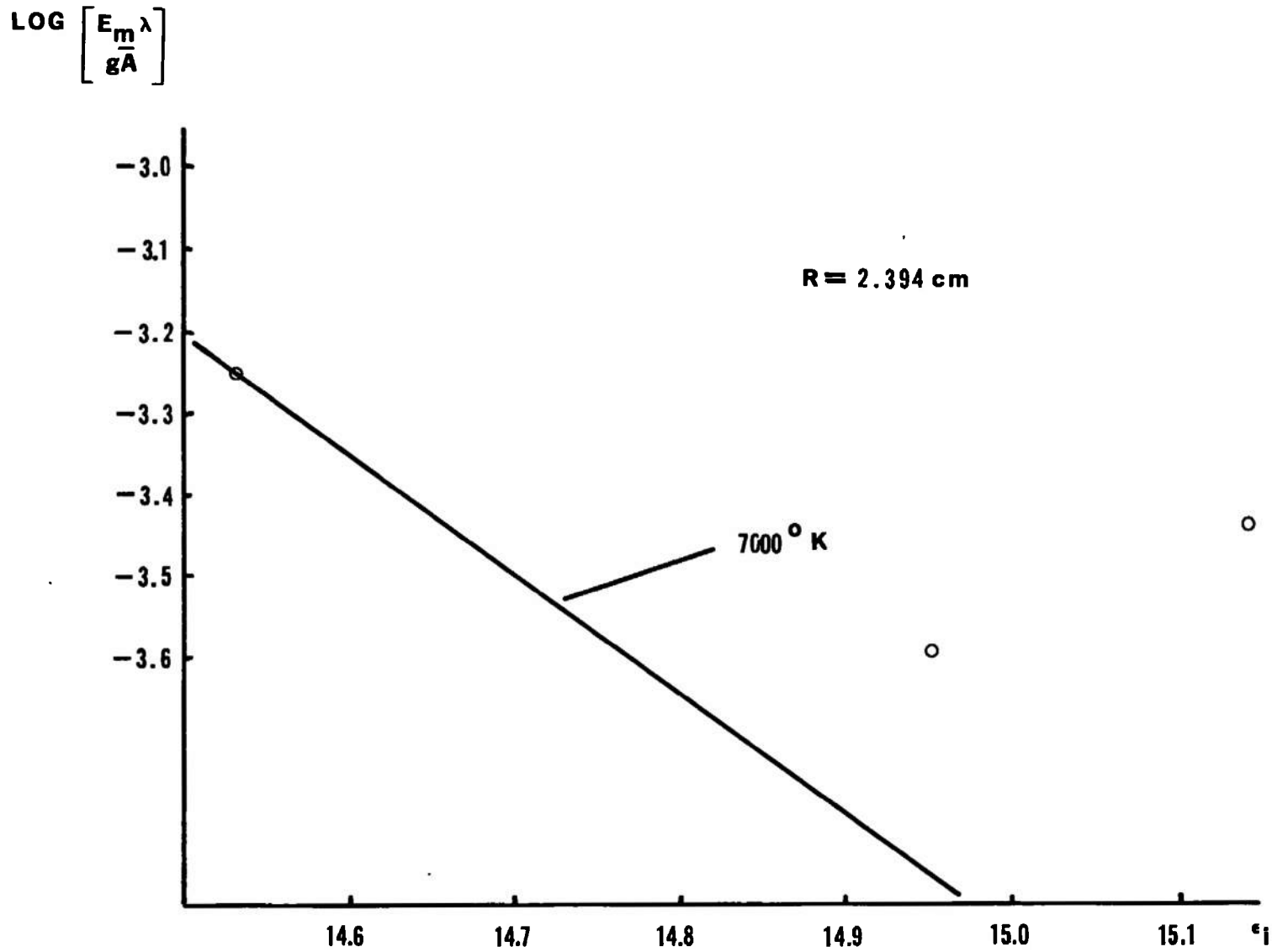

Fig. 15. Boltzmann plot at a radius of 2.394 cm.

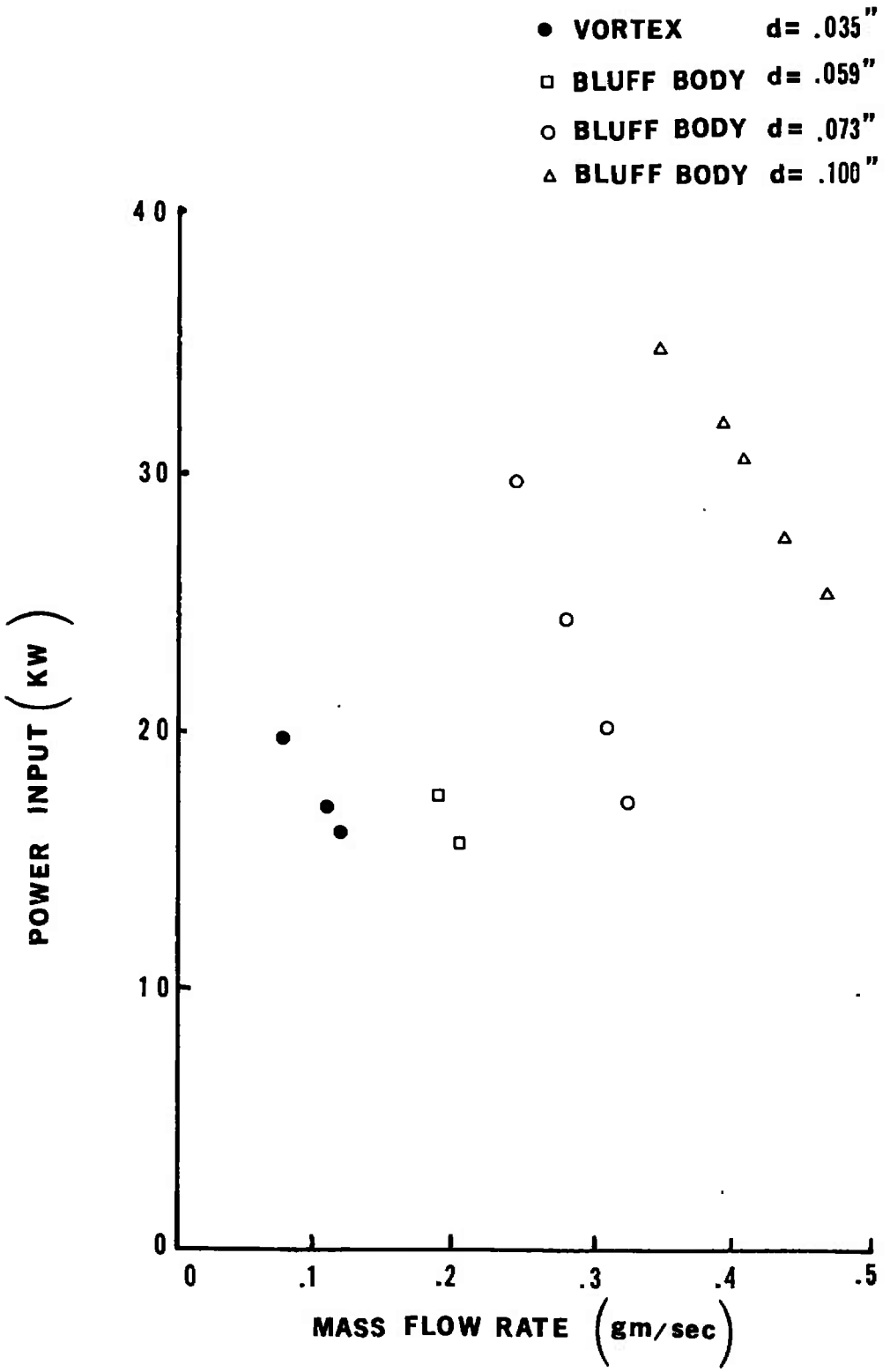

Fig. 16. Input power as a function of flow rate.

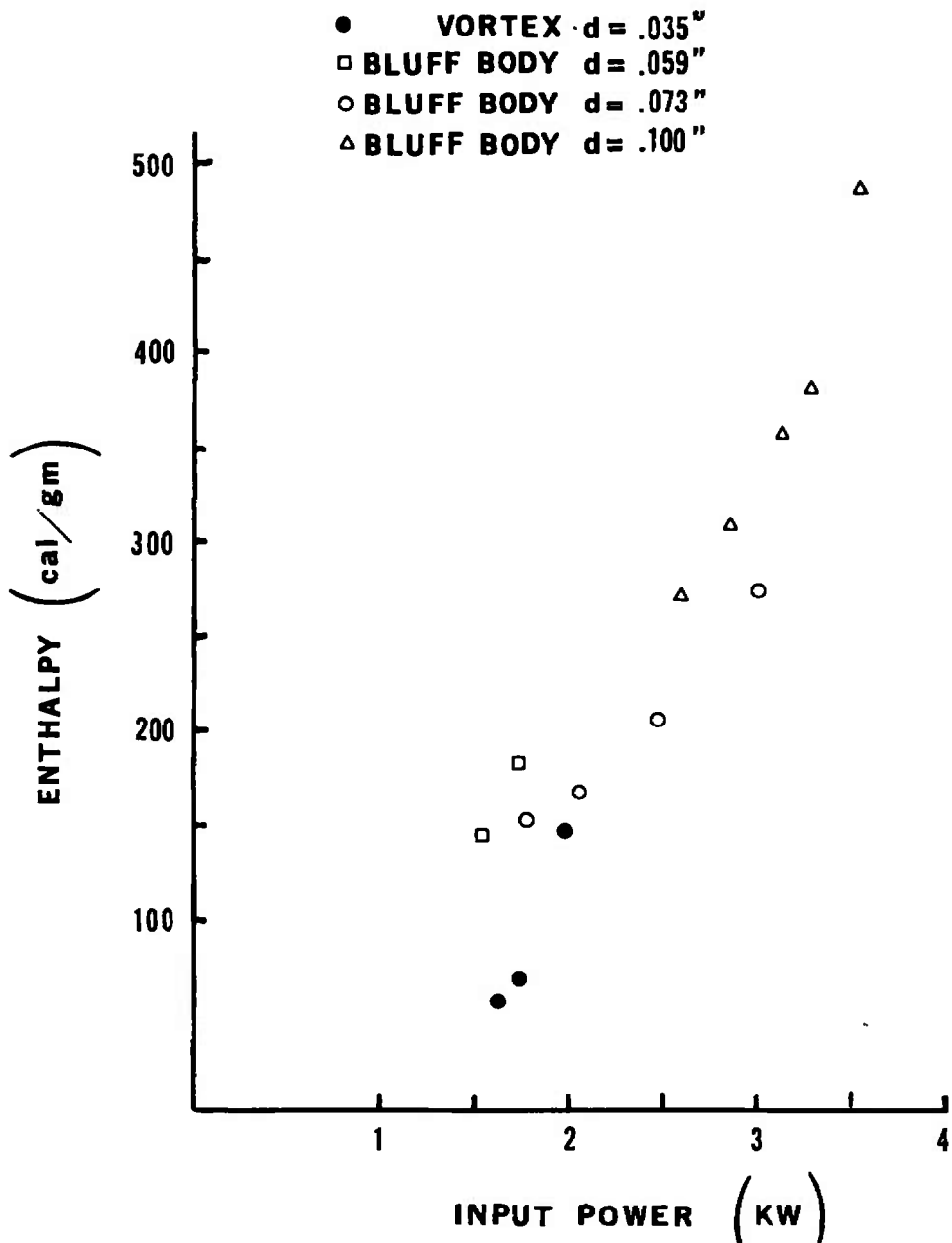

Fig. 17. Enthalpy as a function of input power.

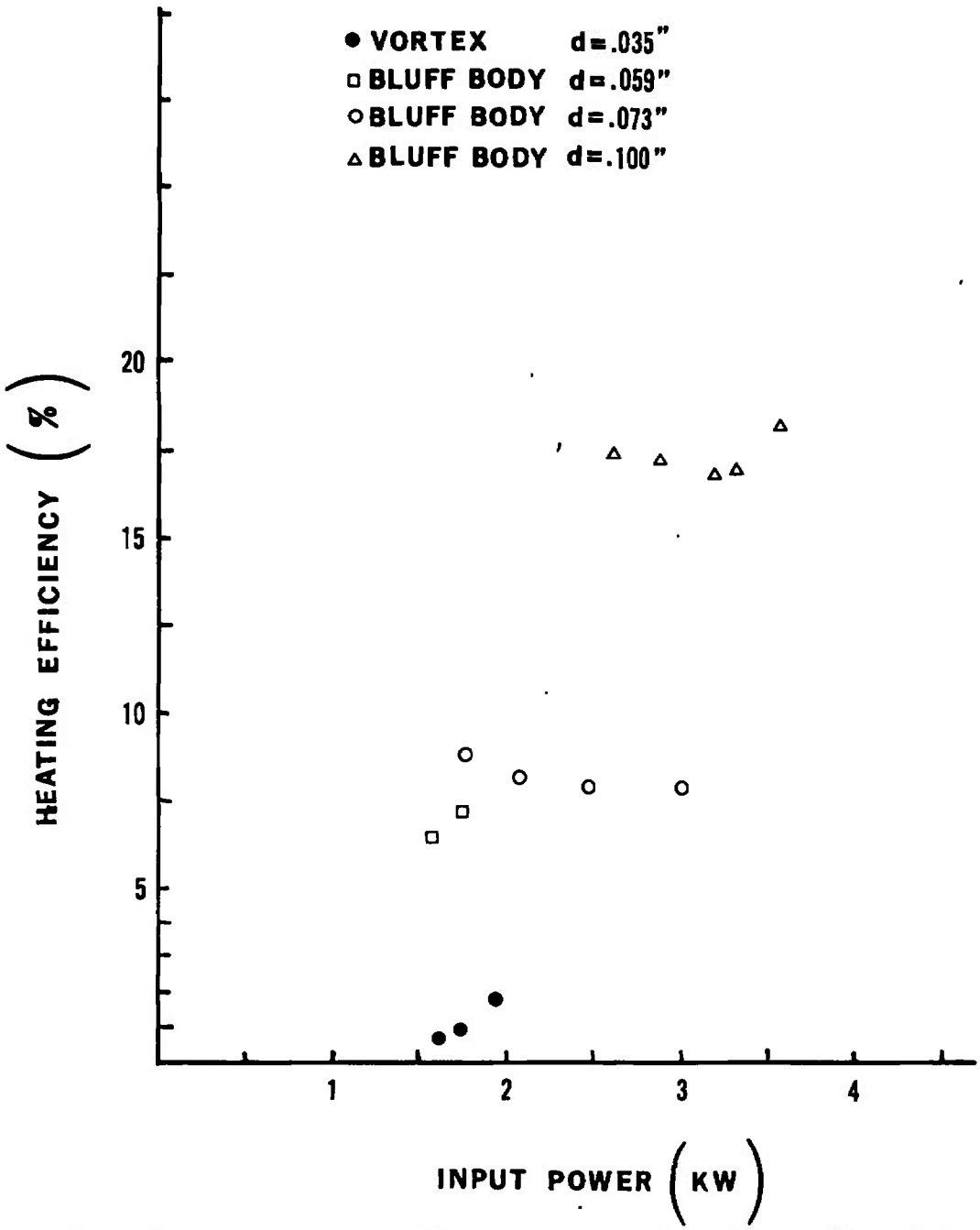

Fig. 18. Heating efficiency as a function of input power.

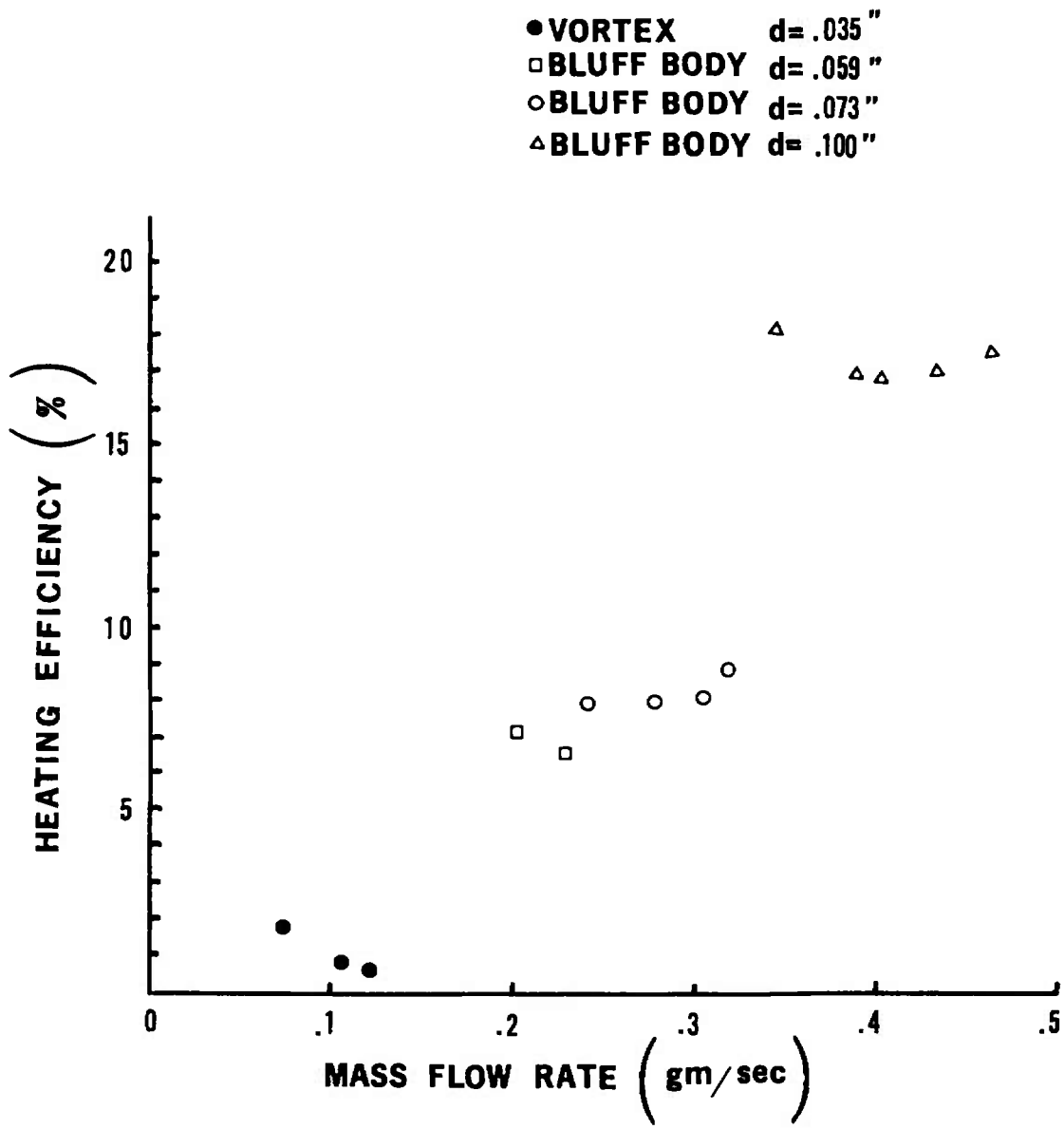

Fig. 19. Heating efficiency as a function of flow rate.

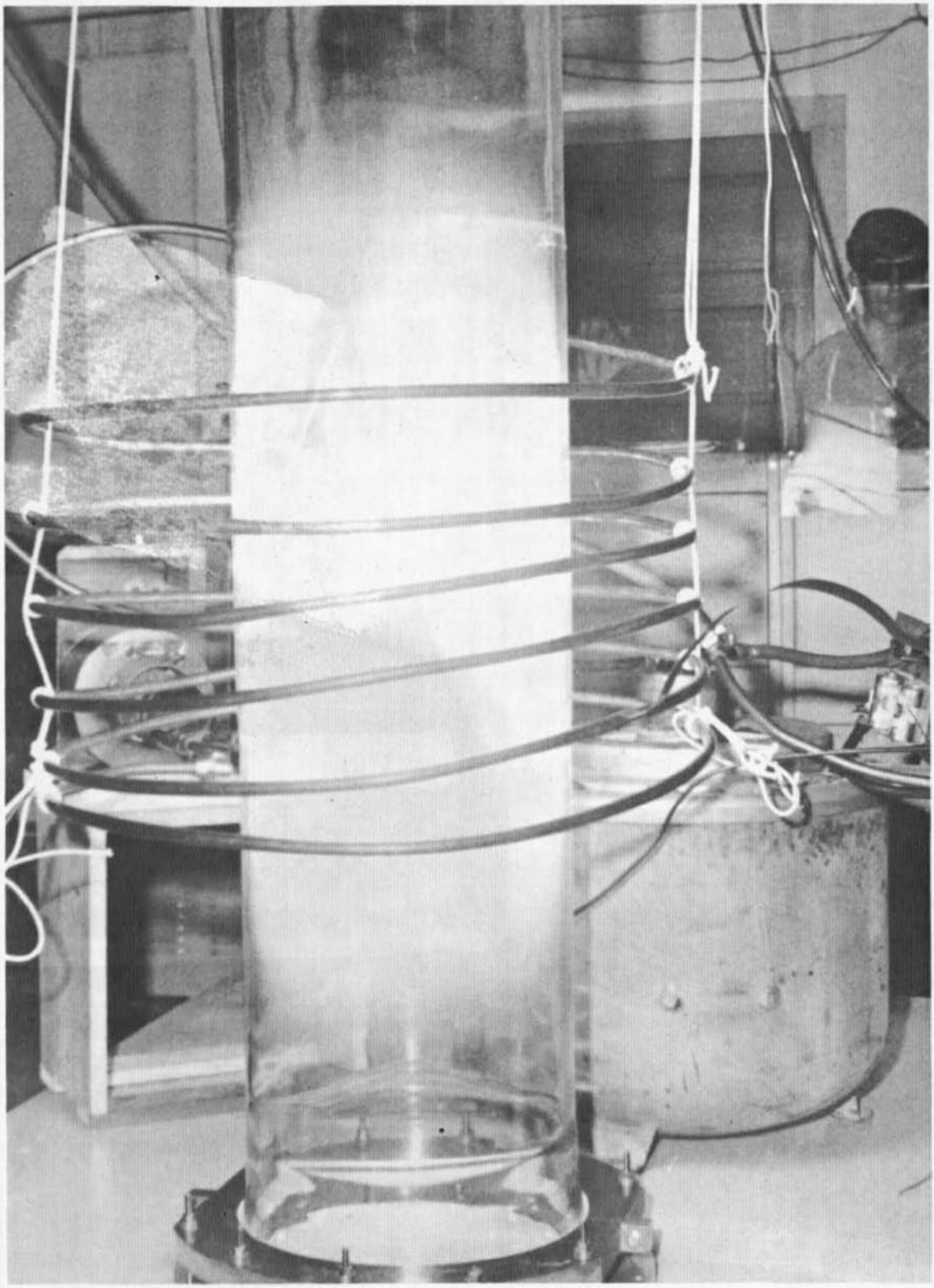

Fig. 20. Twelve inch diameter discharge at low pressure.

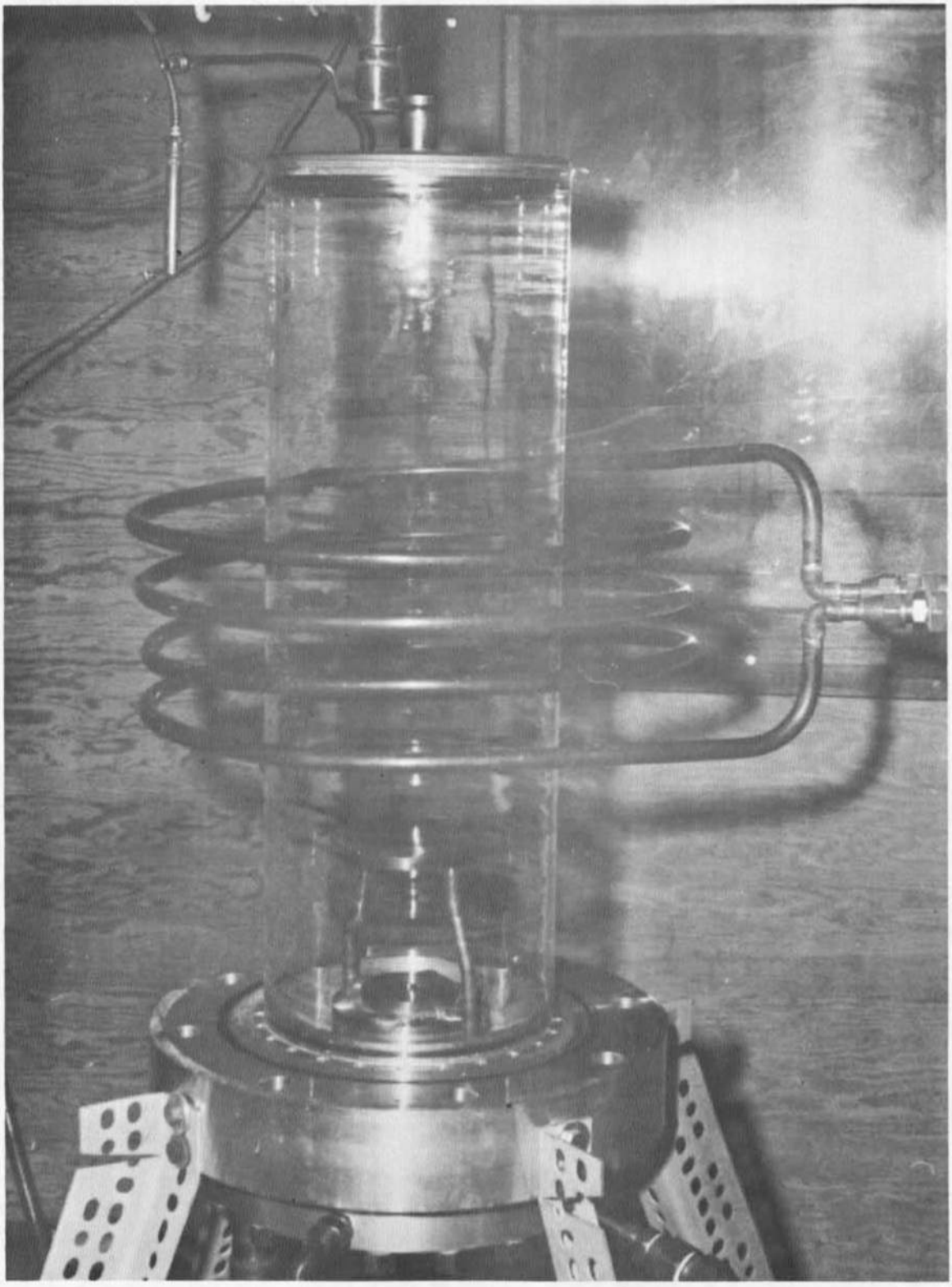

Fig. 21. Photograph of the 7 1/2 inch diameter high pressure discharge chamber with the fiber glass tube removed.

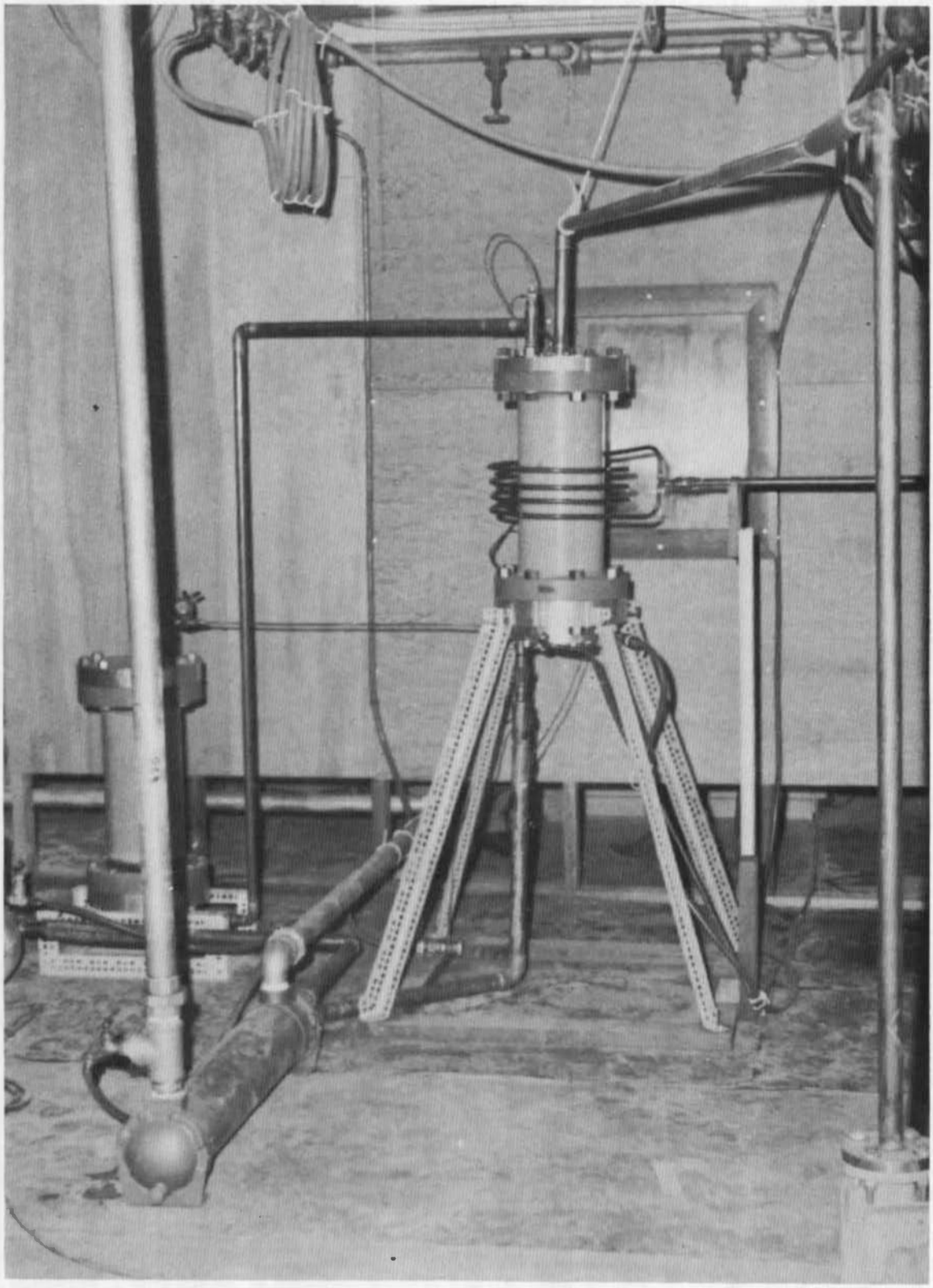

Fig. 22. Photograph of the high pressure discharge system.

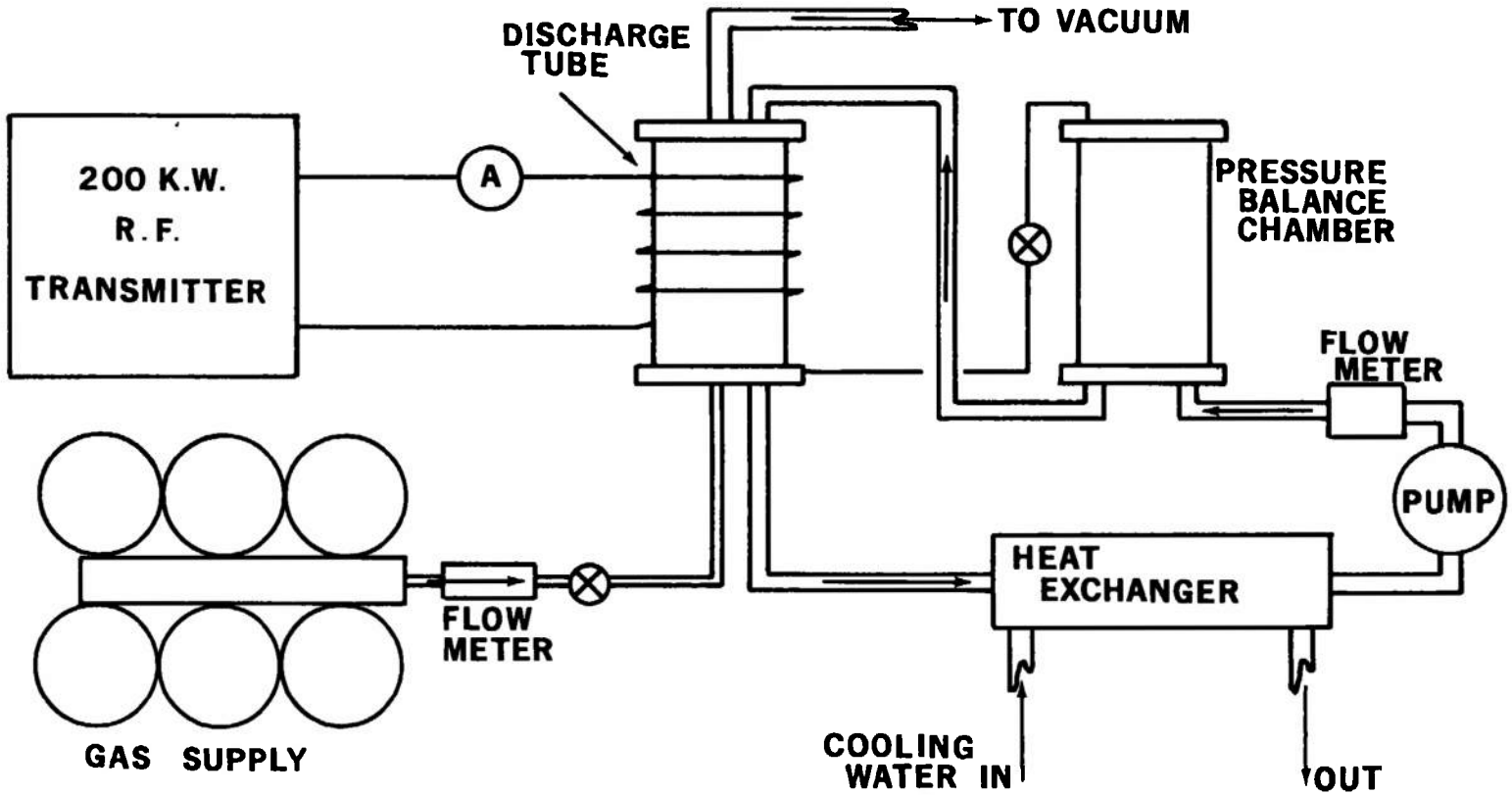

Fig. 23. Schematic representation of the high pressure discharge system.

UNCLASSIFIED

Security Classification

DOCUMENT CONTROL DATA - R & D

(Security classification of title, body of abstract and indexing annotation must be entered when the overall report is classified)

1. ORIGINATING ACTIVITY *(Corporate author)*
University of Florida
Gainesville, Florida

2a. REPORT SECURITY CLASSIFICATION
UNCLASSIFIED

2b. GROUP
N/A

3. REPORT TITLE
AN EXPERIMENTAL STUDY OF ELECTRODELESS ARC DISCHARGES

4. DESCRIPTIVE NOTES *(Type of report and inclusive dates)*
Final Report - November 1969 to January 1971

5. AUTHOR(S) *(First name, middle initial, last name)*
Dennis R. Keefer

6. REPORT DATE	7a. TOTAL NO. OF PAGES	7b. NO. OF REFS
September 1971	67	14

8a. CONTRACT OR GRANT NO.
F40600-70-C-0003

b. PROJECT NO. 8952

c. Program Element 62201F

d. Task 08

9a. ORIGINATOR'S REPORT NUMBER(S)
AEDC-TR-71-180

9b. OTHER REPORT NO(S) *(Any other numbers that may be assigned this report)*
N/A

10. DISTRIBUTION STATEMENT
Approved for public release; distribution unlimited.

11. SUPPLEMENTARY NOTES
Available in DDC

12. SPONSORING MILITARY ACTIVITY
Arnold Engineering Development Center, Air Force Systems Command, Arnold AF Station, Tennessee 37389

13. ABSTRACT An experimental study of electrodeless discharges, stabilized in a flowing stream, has shown that a substantial improvement in stability can be accomplished by the use of a bluff body placed in the entering flow. The increased stability is attributed to energy convection by the circulation cell formed in the wake of the bluff body. Spectroscopic measurements indicate that a more uniform temperature profile is produced as a result of the convective mixing. Detailed measurements indicate that a stable discharge can be maintained with flow rates 3 times greater than is possible with vortex stabilization. It was further determined that the gas heating efficiency of the device is increased by an order of magnitude when compared to the vortex stabilized discharge. The efficiency was found to increase with both power input and flow rate with no indication of a leveling off up to the maximum of 18% measured in the course of the study. A large discharge chamber was constructed to permit operation at pressures to ten atmospheres and input powers to 400 KW, but only preliminary experiments were performed.

DD FORM 1 NOV 65 1473

UNCLASSIFIED

Security Classification

14. KEY WORDS	LINK A		LINK B		LINK C	
	ROLE	WT	ROLE	WT	ROLE	WT
1 electric arcs						
electric discharges						
stability						
2 spectroscopy						
measurement						
plasmas (physics)						

3. Electrodeless arcs 1

AFSC
Arnold AFS Tenn